



PUC
RIO



Engineering the electronic and spintronic properties of graphene by spin-orbit coupling and periodic vacancies

Tese de Doutorado

Matheus Sousa

Outline

- Magneto-electric torque and edge currents
- Engineering nodal lines in the band structure of graphene by periodic vacancies
- Flat-bands in vacancy-engineered structures
- Quantum metric and fidelity number of Dirac materials
- Opacity of graphene

Graphene model

We describe the Graphene as tight-binding model [1]

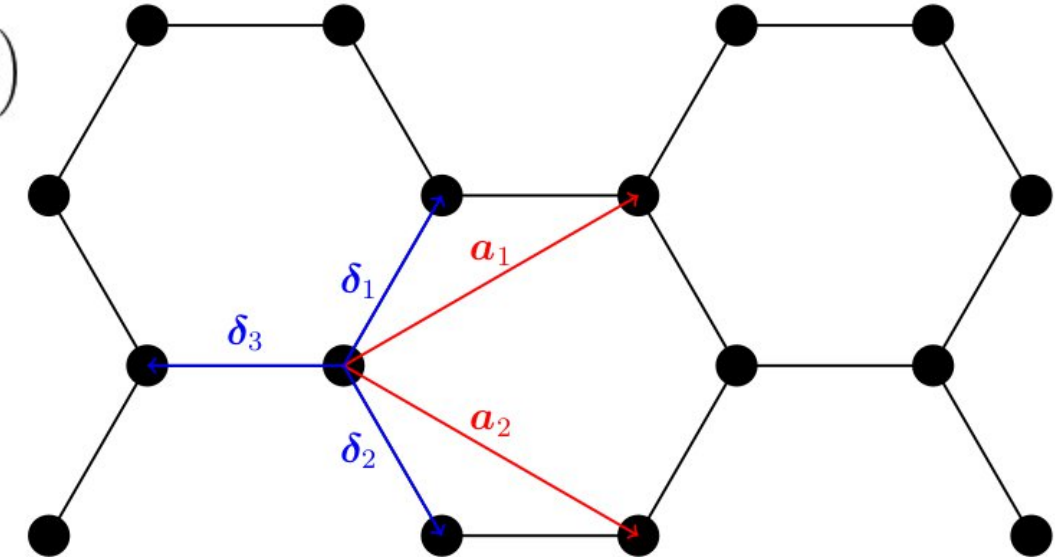
Lattice vectors: $\mathbf{a}_1 = \frac{a}{2} (3, \sqrt{3})$, $\mathbf{a}_2 = \frac{a}{2} (3, -\sqrt{3})$

Reciprocal lattice vectors:

$$\mathbf{b}_1 = \frac{2\pi}{3a} (1, \sqrt{3}), \quad \mathbf{b}_2 = \frac{2\pi}{3a} (1, -\sqrt{3})$$

Nearest-neighbors vectors:

$$\boldsymbol{\delta}_1 = \frac{a}{2} (1, \sqrt{3}), \quad \boldsymbol{\delta}_2 = \frac{a}{2} (1, -\sqrt{3}), \quad \boldsymbol{\delta}_3 = -a (1, 0)$$



Graphene crystal structure

Tight-binding Hamiltonian: $H = -t \sum_{\langle ij \rangle \sigma} c_{i\sigma}^\dagger c_{j\sigma} + \text{h.c.}$

[1] Neto, A. C., Guinea, F., Peres, N. M., Novoselov, K. S., & Geim, A. K. (2009). RMP, 81(1), 109.

Graphene Model with RSOC and Magnetization

We include Rashba spin-orbit

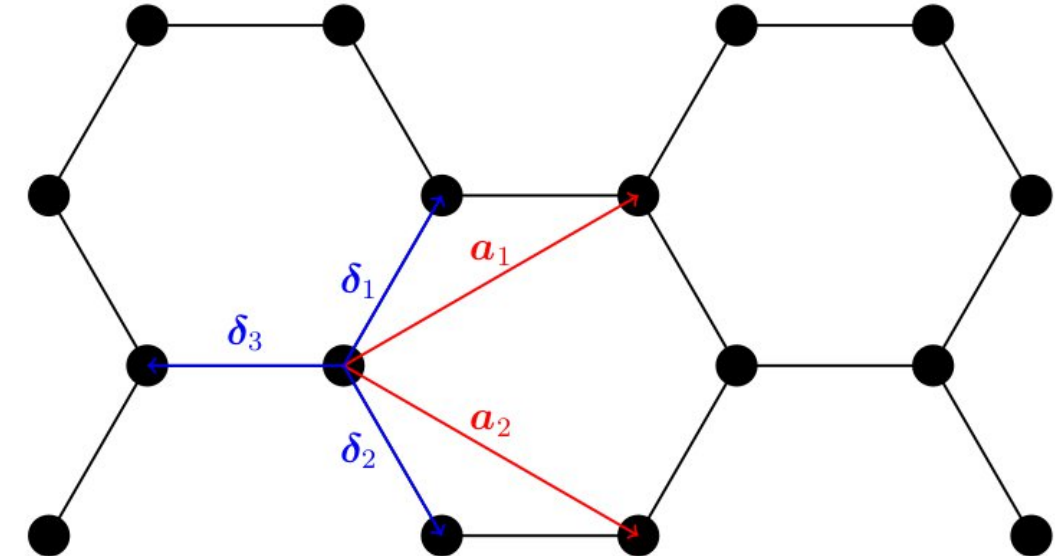
$$H_{RSOC} = i\lambda_R \sum_{\langle ij \rangle \alpha\beta} c_{i\alpha}^\dagger (\boldsymbol{\sigma}_{\alpha\beta} \times \mathbf{d}_{ij})^z c_{j\beta} + \text{h.c.}$$

and exchange coupling

$$H_{ex} = J_{ex} \sum_{i\alpha\beta} \mathbf{S} \cdot c_{i\alpha}^\dagger \boldsymbol{\sigma}_{\alpha\beta} c_{i\beta} + \text{h.c.}$$

Considering an extended tightbinding model:

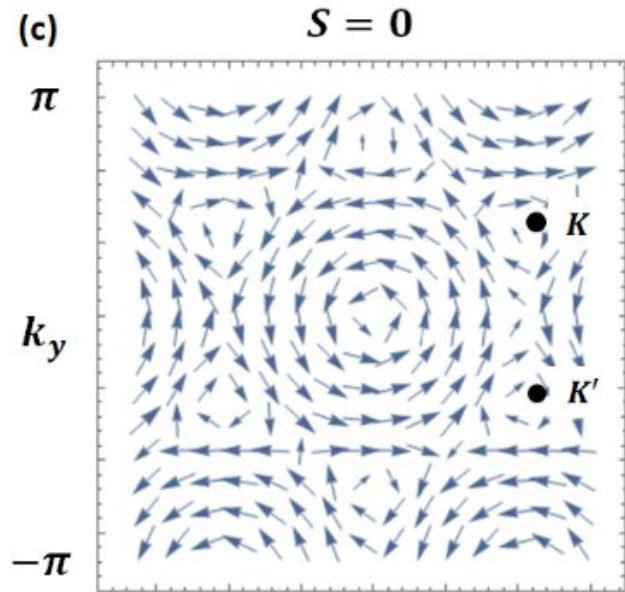
$$\begin{aligned} H = & -\mu \sum_{i\sigma} c_{i\sigma}^\dagger c_{i\sigma} - t \sum_{\langle ij \rangle} c_{i\uparrow}^\dagger c_{j\uparrow} \\ & + i\lambda_R \sum_{\langle ij \rangle \alpha\beta} c_{i\alpha}^\dagger \boldsymbol{\sigma}_{\alpha\beta} c_{j\beta} + J_{ex} \sum_{i\alpha\beta} \mathbf{S} \cdot c_{i\alpha}^\dagger \boldsymbol{\sigma}_{\alpha\beta} c_{i\beta} + \text{h.c.} \end{aligned}$$



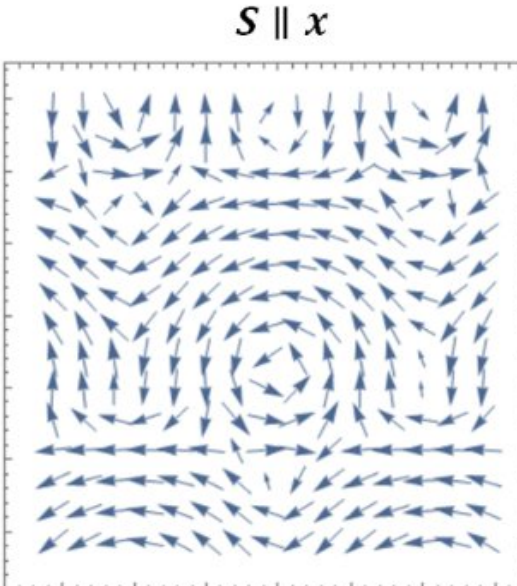
Graphene crystal structure

Equilibrium currents in Graphene

We investigate the spin profile in the presence of RSOC



Spin-momentum locking
with $S=0$



Spin momentum locking
with S parallel to x

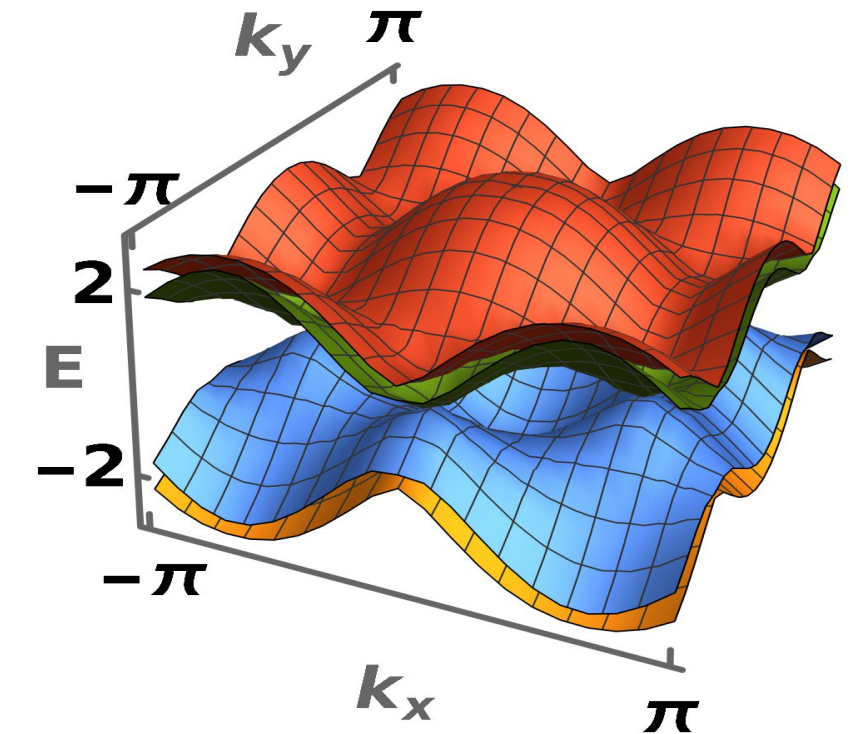
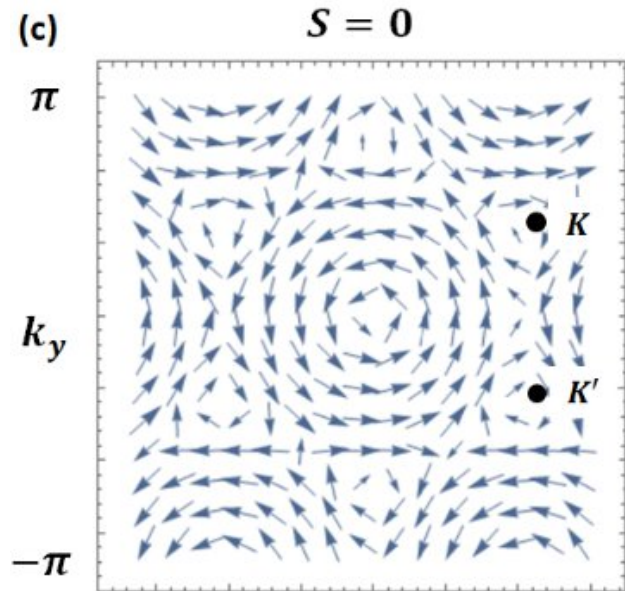


Fig. Band structure of
graphene with RSOC

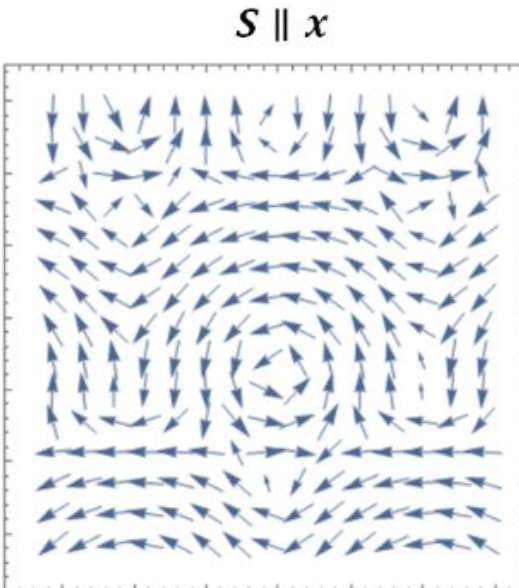
$$H = -\mu \sum_{i\sigma} c_{i\sigma}^\dagger c_{i\sigma} - t \sum_{\langle ij \rangle} c_{i\uparrow}^\dagger c_{j\uparrow}$$
$$+ i\lambda_R \sum_{\langle ij \rangle \alpha\beta} c_{i\alpha}^\dagger \boldsymbol{\sigma}_{\alpha\beta} c_{j\beta} + J_{ex} \sum_{i\alpha\beta} \mathbf{S} \cdot c_{i\alpha}^\dagger \boldsymbol{\sigma}_{\alpha\beta} c_{i\beta} + \text{h.c.}$$

Equilibrium currents in Graphene

We investigate the spin profile in the presence of RSOC



Spin-momentum locking
with $S=0$



Spin momentum locking
with S parallel to x

$$H = -\mu \sum_{i\sigma} c_{i\sigma}^\dagger c_{i\sigma} - t \sum_{\langle ij \rangle} c_{i\uparrow}^\dagger c_{j\uparrow}$$
$$+ i\lambda_R \sum_{\langle ij \rangle \alpha\beta} c_{i\alpha}^\dagger \boldsymbol{\sigma}_{\alpha\beta} c_{j\beta} + J_{ex} \sum_{i\alpha\beta} \mathbf{S} \cdot c_{i\alpha}^\dagger \boldsymbol{\sigma}_{\alpha\beta} c_{i\beta} + \text{h.c.}$$

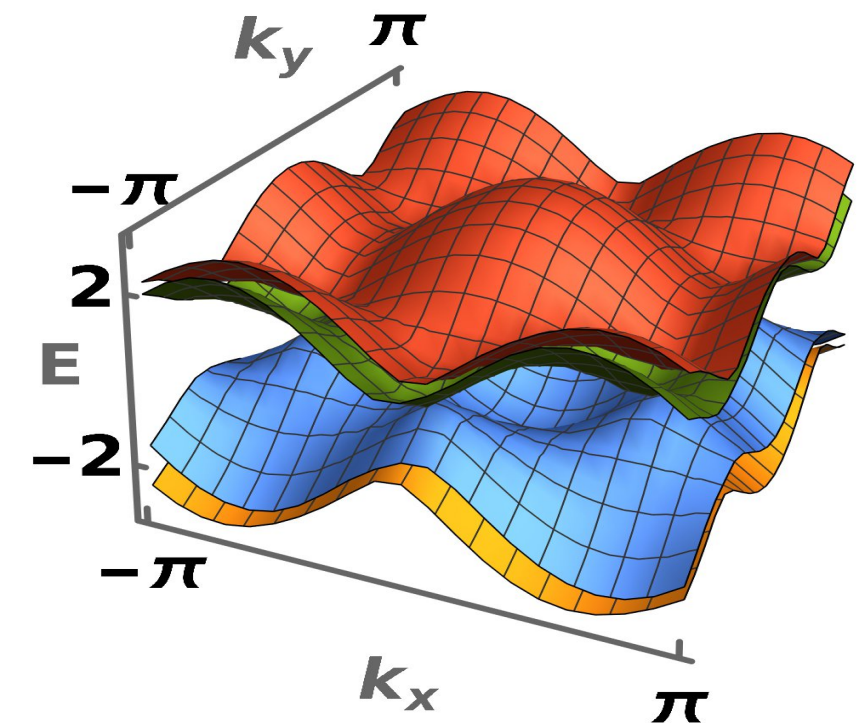
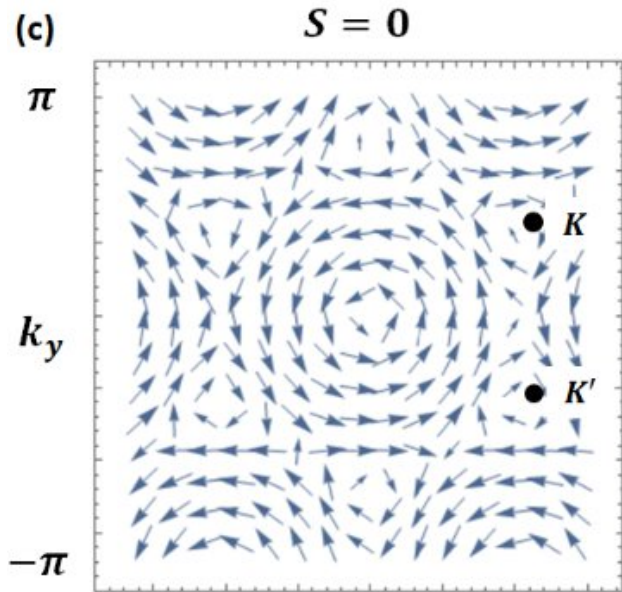


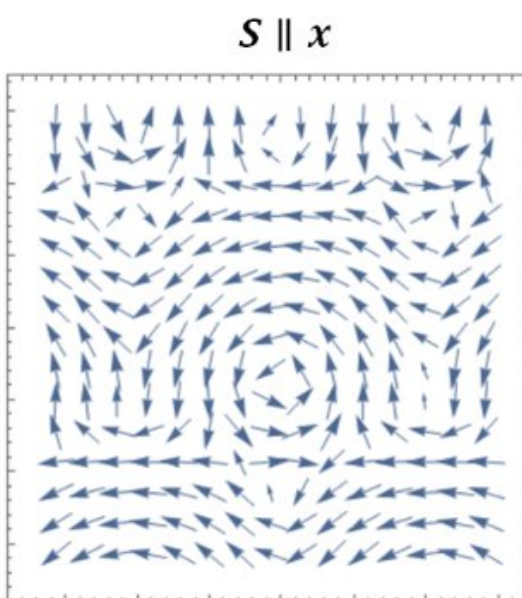
Fig. Band structure of
graphene with RSOC and
magnetization

Equilibrium currents in Graphene

We investigate the spin profile in the presence of RSOC



Spin-momentum locking
with $S=0$



Spin momentum locking
with S parallel to x

$$H = -\mu \sum_{i\sigma} c_{i\sigma}^\dagger c_{i\sigma} - t \sum_{\langle ij \rangle} c_{i\uparrow}^\dagger c_{j\uparrow}$$
$$+ i\lambda_R \sum_{\langle ij \rangle \alpha\beta} c_{i\alpha}^\dagger \boldsymbol{\sigma}_{\alpha\beta} c_{j\beta} + J_{ex} \sum_{i\alpha\beta} \mathbf{S} \cdot c_{i\alpha}^\dagger \boldsymbol{\sigma}_{\alpha\beta} c_{i\beta} + \text{h.c.}$$

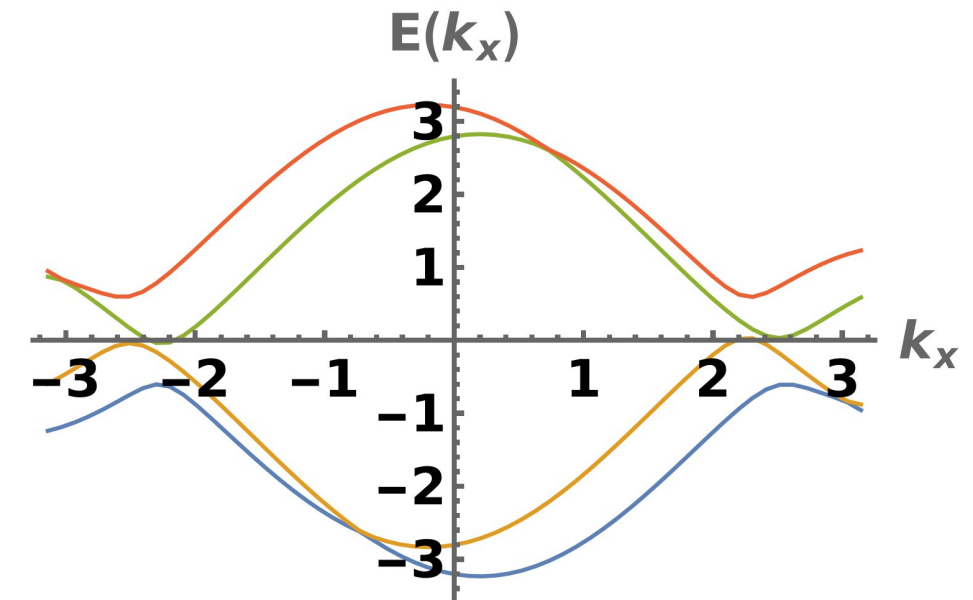


Fig. Band structure of
graphene with RSOC and
magnetization

Equilibrium currents in Graphene

Continuity equation formalism:

For charge current:

$$\begin{aligned}\dot{n}_i &= \frac{i}{\hbar} [H, n_i] = \frac{i}{\hbar} [H_t + H_R, n_i] \\ &= -\nabla \cdot \mathbf{J}_i^0 = -\frac{1}{a} \sum_{\eta} J_{i,i+\eta}^0,\end{aligned}$$

For spin current:

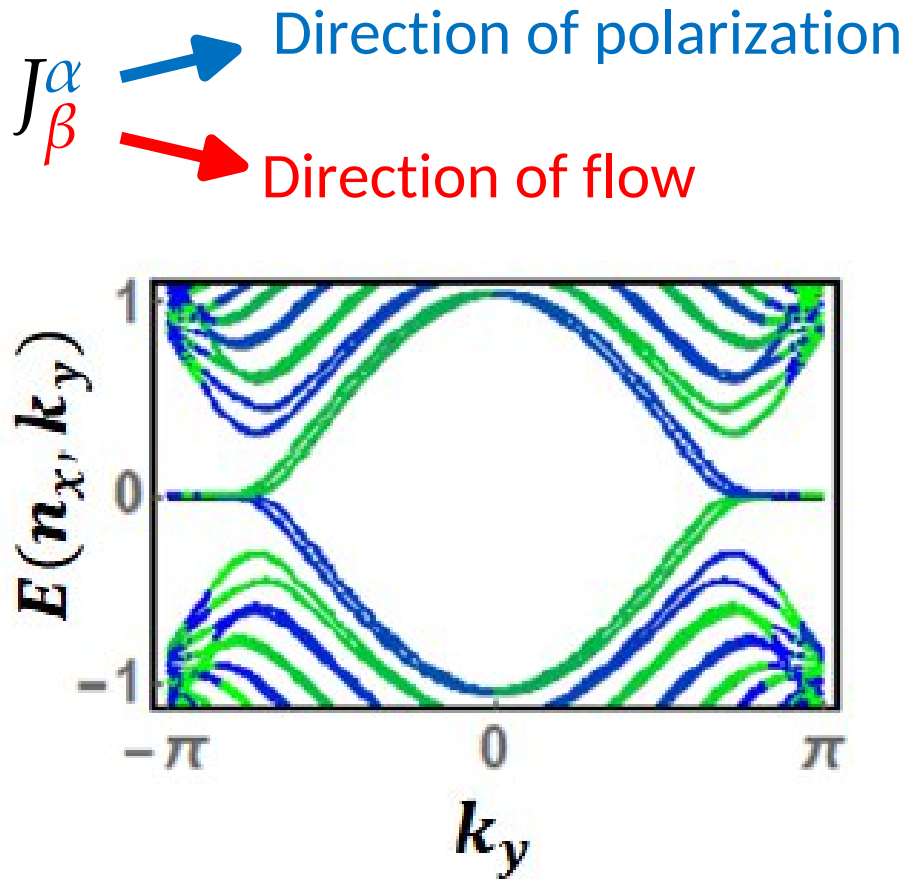
$$\begin{aligned}\dot{m}_i^a &= \frac{i}{\hbar} [H, m_i^a] = \frac{i}{\hbar} [H_t + H_R, m_i^a] + \frac{i}{\hbar} [H_J, m_i^a] \\ &= -\nabla \cdot \mathbf{J}_i^a + \tau_i^a \\ &= -\frac{1}{a} \sum_{\eta} J_{i,i+\eta}^a + \frac{2J_{ex}}{\hbar} (\mathbf{S} \times c_{i\alpha} \boldsymbol{\sigma}_{\alpha\beta} c_{i\beta})^a,\end{aligned}$$

Spin torque:

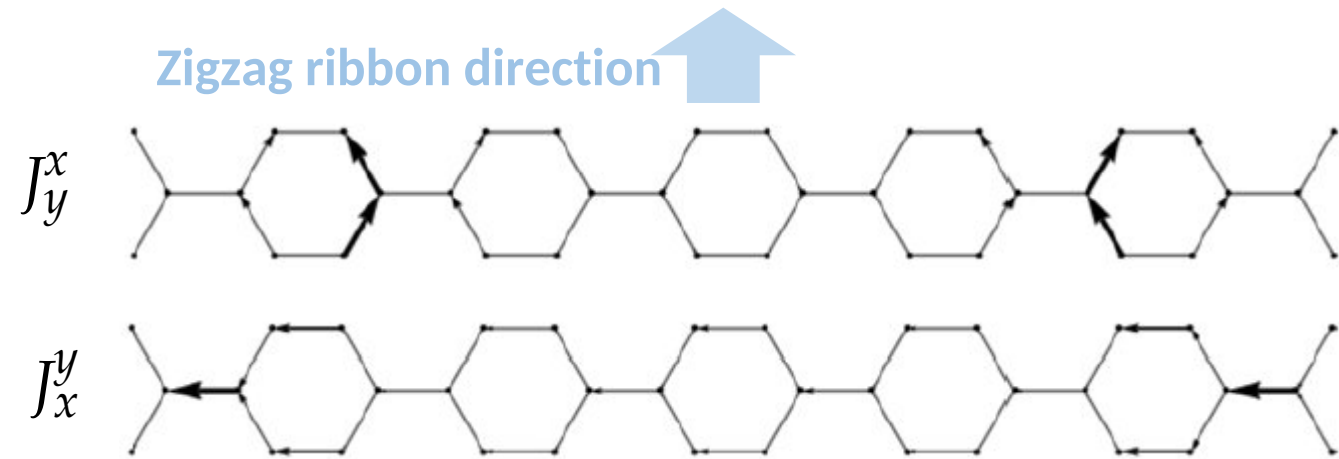
$$\tau_i^a = \frac{2J_{ex}}{\hbar} (\mathbf{S} \times c_{i\alpha} \boldsymbol{\sigma}_{\alpha\beta} c_{i\beta})^a$$

Chiral edge spin current in GNRs

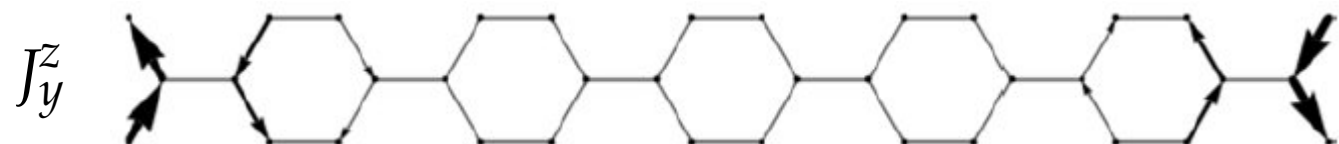
Following spin-current notation:



- RSOC alone is known to cause bulk in-plane spin-current [1]



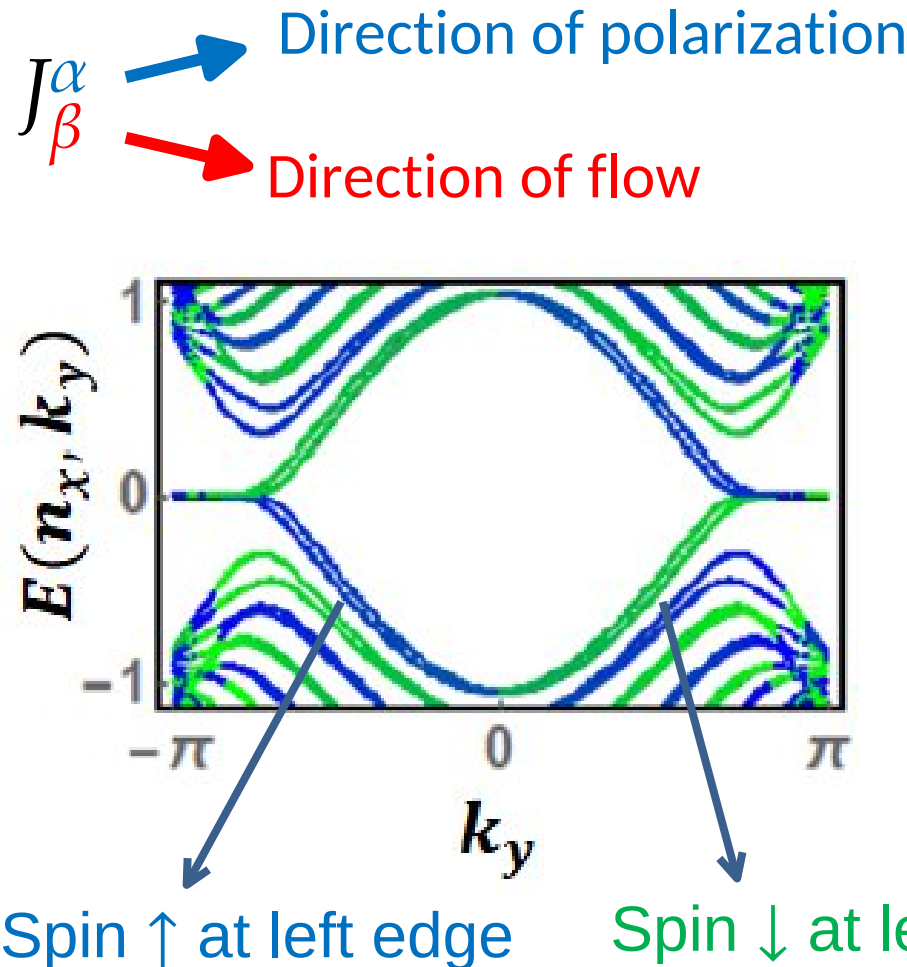
We also find out-of-plane polarized chiral edge spin current



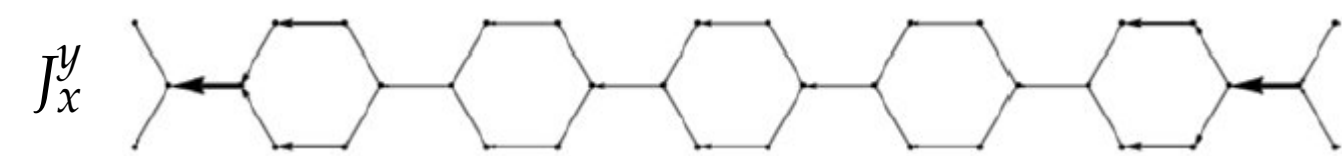
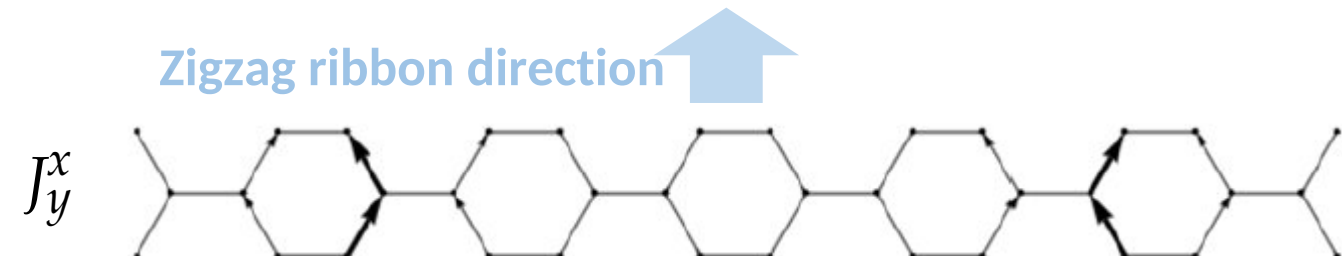
[1] Rashba, E.I. (2003). Physical Review B, 68, 241315.

Chiral edge spin current in GNRs

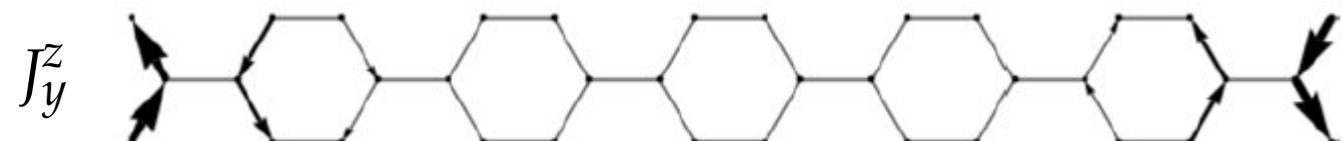
Following spin-current notation:



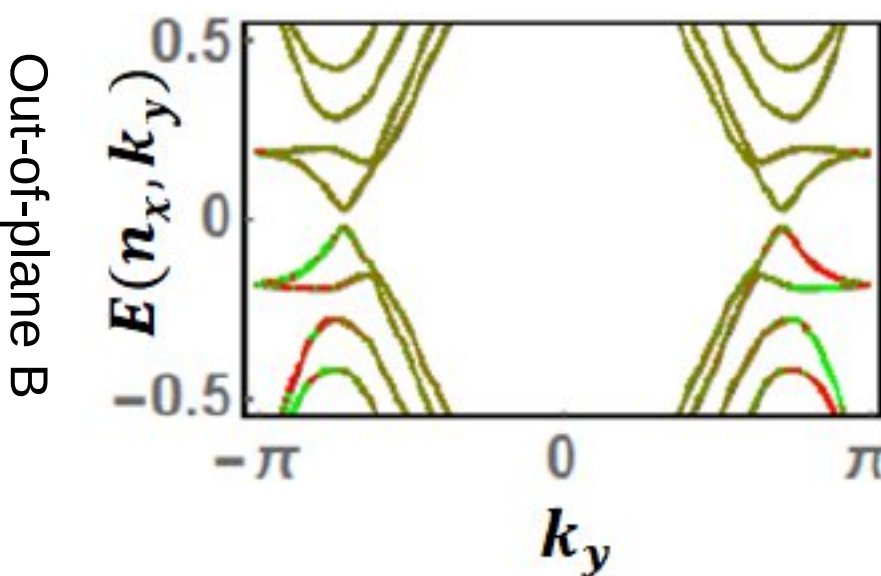
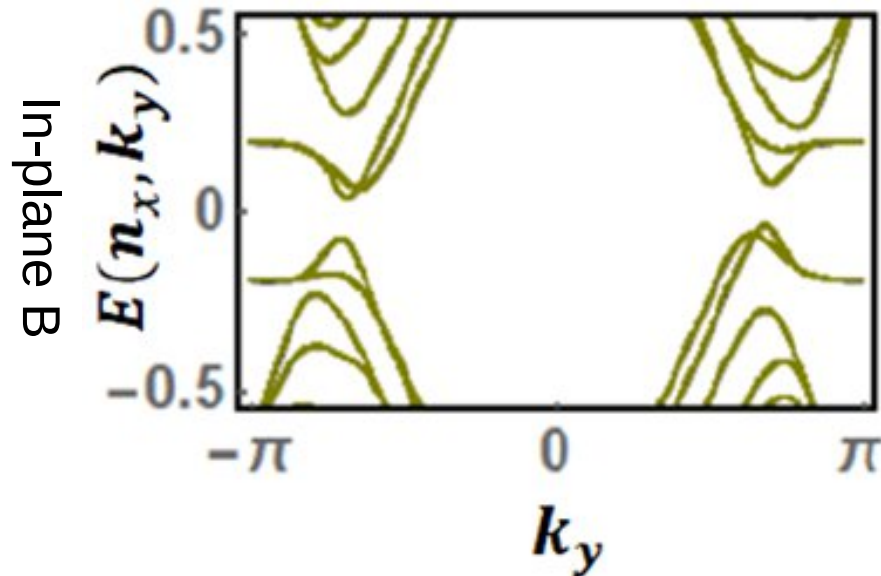
- RSOC alone is known to cause bulk in-plane spin-current [1]



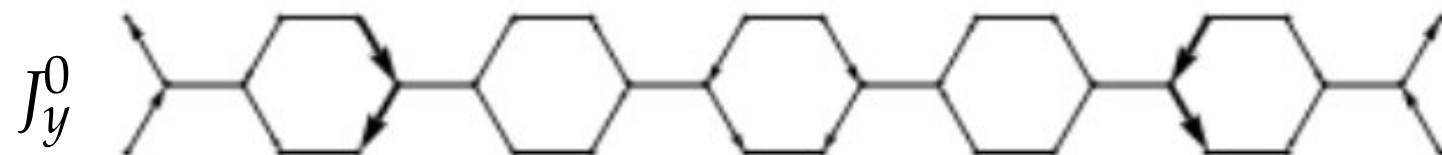
We also find out-of-plane polarized chiral edge spin current



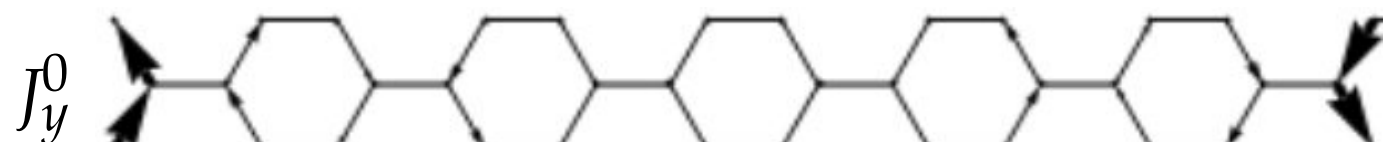
Charge currents in GNRs with Magnetization



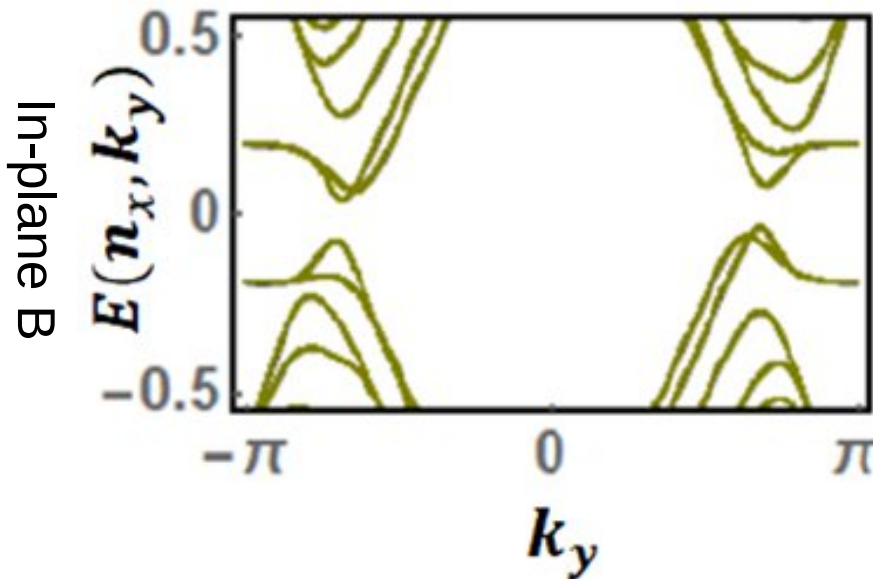
Asymmetric band structure due to magnetization leading to non-chiral edge charge current symmetric between the two edges



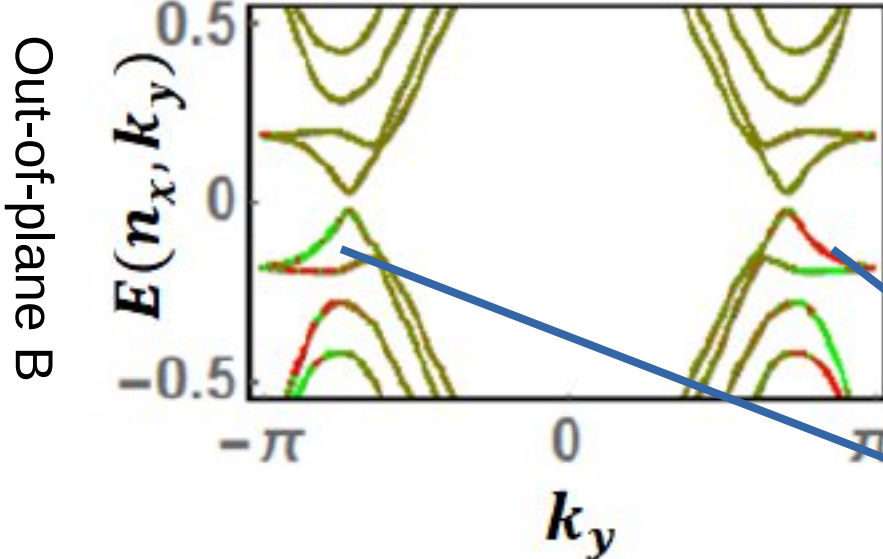
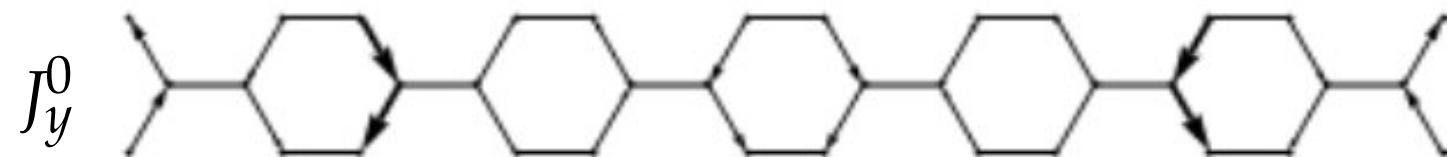
The spin polarization of the band structure indicates the chirality of the edge current



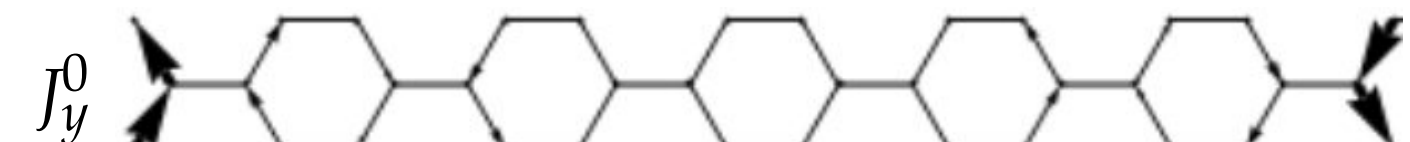
Charge currents in GNRs with Magnetization



Asymmetric band structure due to magnetization leading to non-chiral edge charge current symmetric between the two edges



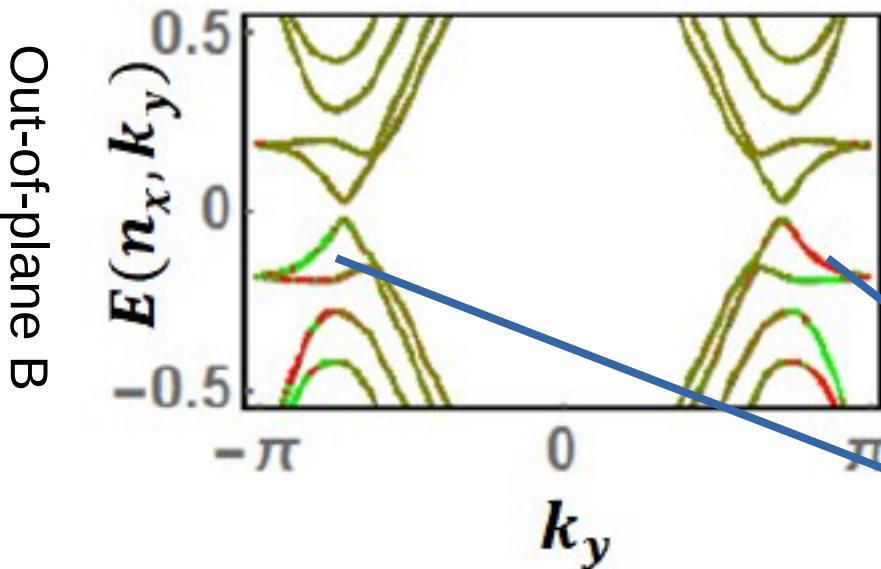
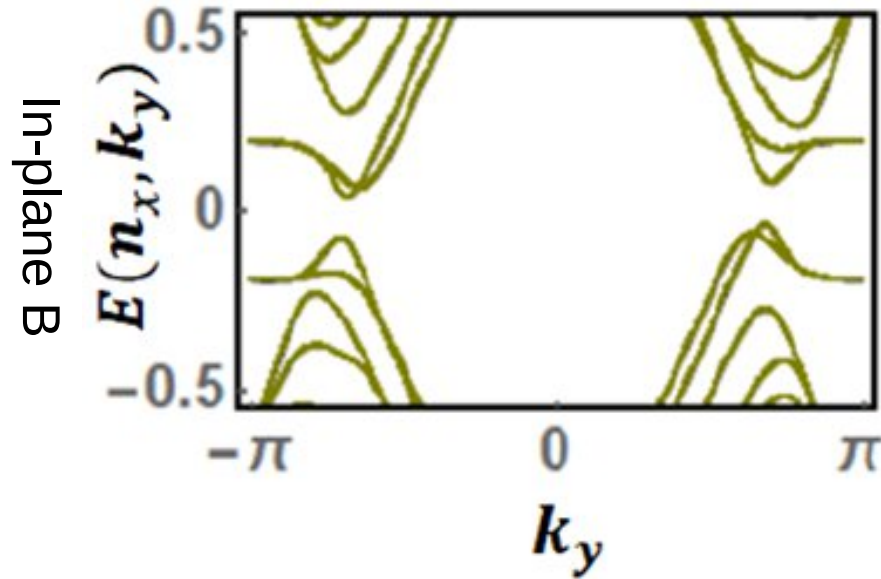
The spin polarization of the band structure indicates the chirality of the edge current



Wave function at left edge

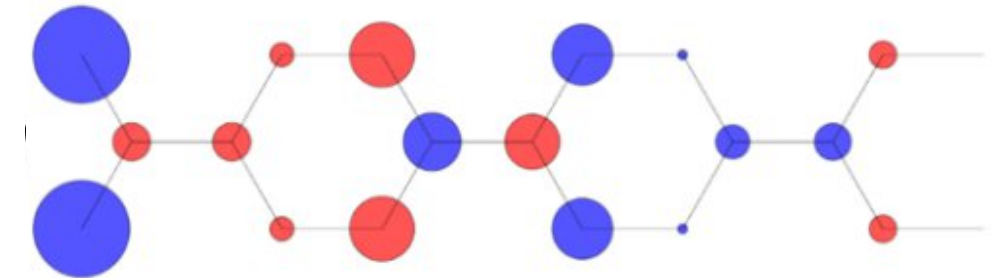
Wave function at right edge

Charge currents in GNRs with Magnetization

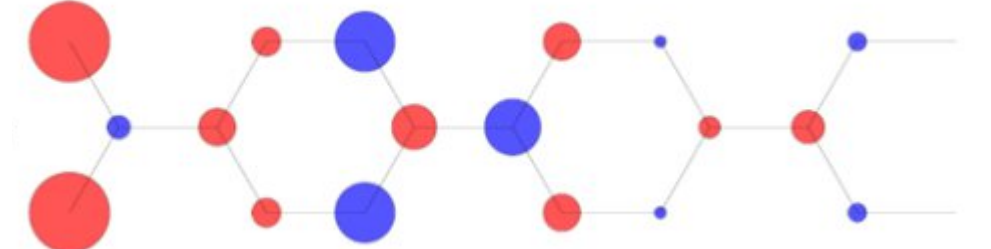


In both cases, a asymmetric transverse spin polarization:

$$\sigma_{AS}^z$$



$$\sigma_{AS}^x$$



Wave function at left edge

Wave function at right edge

Partially magnetized and irregular nanoflakes

- We can induce a local local torque using magnetization
- However, the total torque averages to zero
- To make a spintronics device [1], we need an observable, finite, torque

Partially magnetized and irregular nanoflakes

- We can induce a local local torque using magnetization
- However, the total torque averages to zero
- To make a spintronics device [1], we need an observable, finite, torque

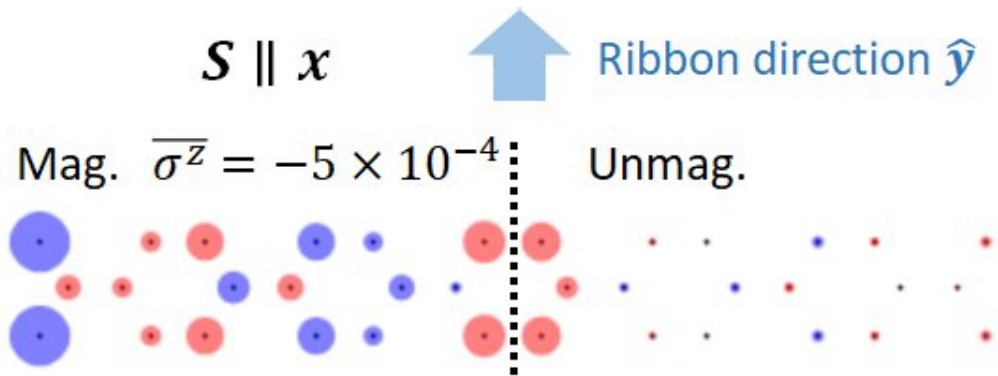


Fig. Partially magnetized sample with finite torque

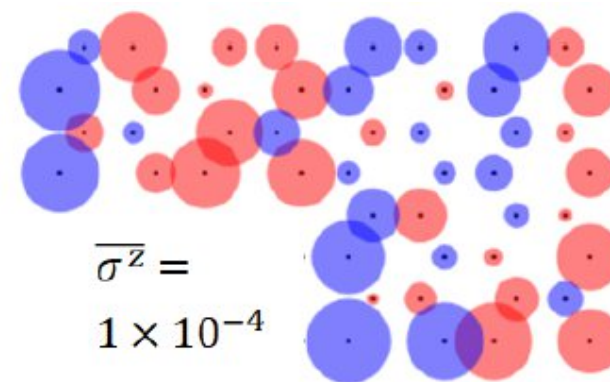


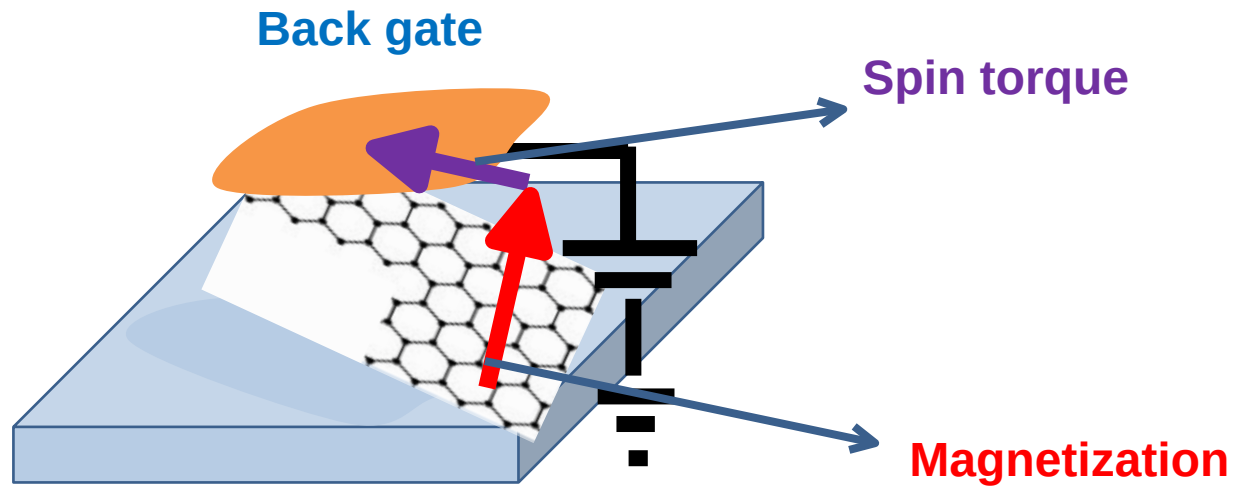
Fig. Irregular nanoflake with finite torque

Significance and potential applications to spintronics

- We could observe similarities with the 2DEG paper from Rashba
- Uncover the chiral, edge, spin-currents in the z-direction. QSHE but with no topology.
- Manipulate the charge-current by tuning the direction of magnetization, chiral or not.
- Transverse spin polarization indicating a local torque.

Significance and potential applications to spintronics

- We could observe similarities with the 2DEG paper from Rashba
- Uncover the chiral, edge, spin-currents in the z-direction. QSHE but with no topology.
- Manipulate the charge-current by tuning the direction of magnetization, chiral or not.
- Transverse spin polarization indicating a local torque.



Introduction to nonsymmorphic symmetries and nodal lines

- In previous papers [1,2], showed that robust nodal lines in borophene with periodic vacancies.
- Using vacancy engineering, we showed the same can occur in graphene.



Fig. Example of glide-plane pattern

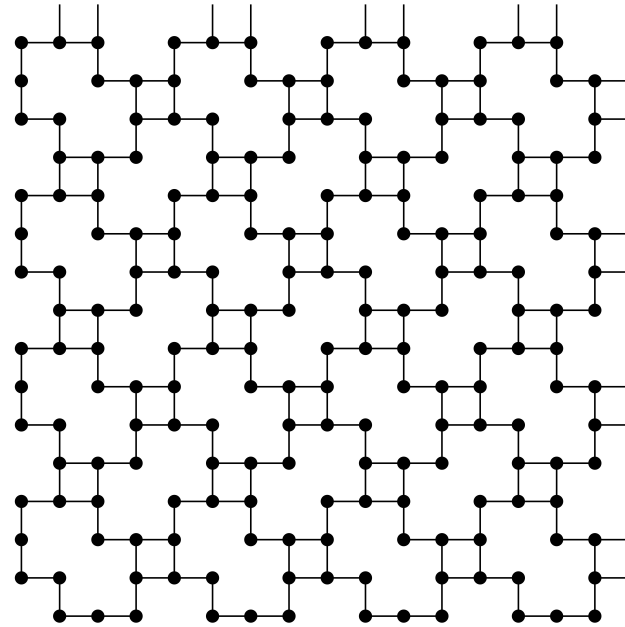


Fig. Example of lattice with
nonsymmorphic symmetry (p4g)

Using periodic vacancies to create nodal lines in Graphene

1D case:

Glide operator:
$$g(k) = \begin{pmatrix} 0 & e^{-ik} \\ 1 & 0 \end{pmatrix}$$

Since it commutes with the Hamiltonian

$$g(k)|\psi_{\pm}(k)\rangle = \pm e^{-ik/2}|\psi_{\pm}(k)\rangle$$

$$H(k)|\psi_{\pm}(k)\rangle = E_{\pm}(k)|\psi_{\pm}(k)\rangle$$

By the symmetry of the glide operator:

$$g(0)|\psi_+(0)\rangle = +|\psi_+(0)\rangle,$$

$$g(0)|\psi_-(0)\rangle = -|\psi_-(0)\rangle,$$

$$g(2\pi)|\psi_+(2\pi)\rangle = +e^{-i\pi}|\psi_+(2\pi)\rangle = -|\psi_+(2\pi)\rangle = g(0)|\psi_+(2\pi)\rangle$$

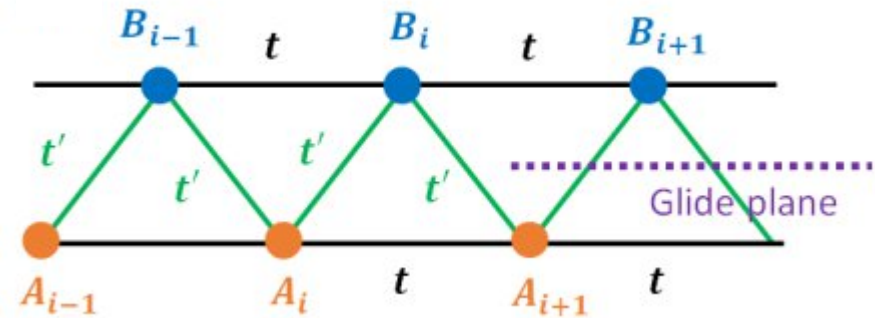


Fig. 1D model with glide symmetry

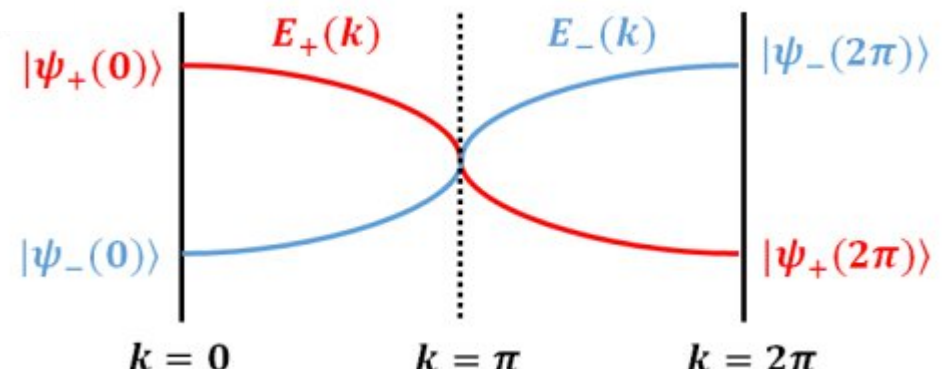


Fig. Eigenstates along the Brillouin Zone

Using periodic vacancies to create nodal lines in Graphene

1D case:

Glide operator: $g(k) = \begin{pmatrix} 0 & e^{-ik} \\ 1 & 0 \end{pmatrix}$

Since it commutes with the Hamiltonian

$$g(k)|\psi_{\pm}(k)\rangle = \pm e^{-ik/2}|\psi_{\pm}(k)\rangle$$

$$H(k)|\psi_{\pm}(k)\rangle = E_{\pm}(k)|\psi_{\pm}(k)\rangle$$

By the symmetry of the glide operator:

$$g(0)|\psi_+(0)\rangle = +|\psi_+(0)\rangle,$$

$$g(0)|\psi_-(0)\rangle = -|\psi_-(0)\rangle,$$

$$g(2\pi)|\psi_+(2\pi)\rangle = +e^{-i\pi}|\psi_+(2\pi)\rangle = -|\psi_+(2\pi)\rangle = g(0)|\psi_+(2\pi)\rangle$$

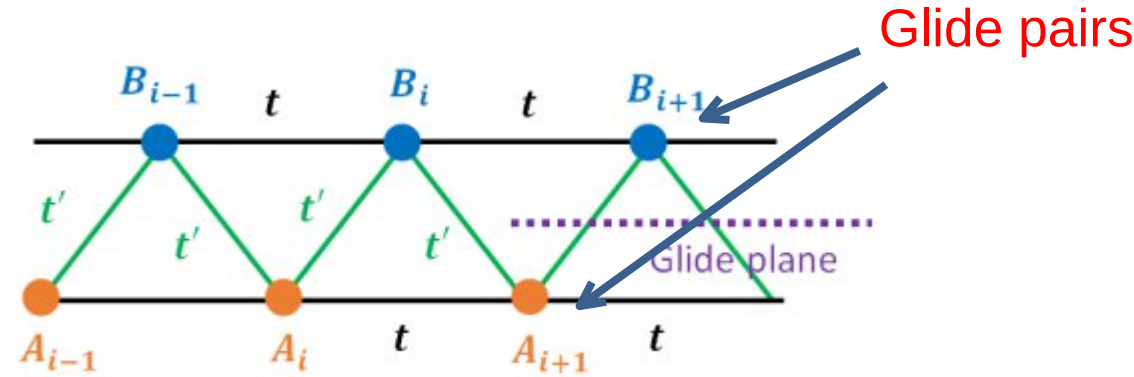


Fig. 1D model with glide symmetry

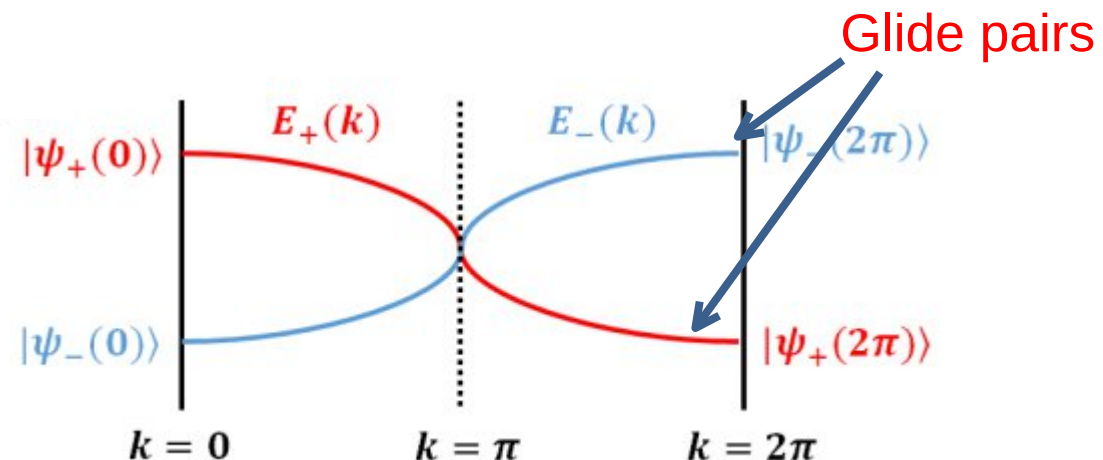


Fig. Eigenstates along the Brillouin Zone

Vacancy engineering technique to create desired symmetries

- Our goal is to create the nonsymmorphic pattern in graphene
- We will do this by using vacancy engineering

Vacancy engineering technique to create desired symmetries

- Our goal is to create the nonsymmorphic pattern in graphene
- We will do this by using vacancy engineering

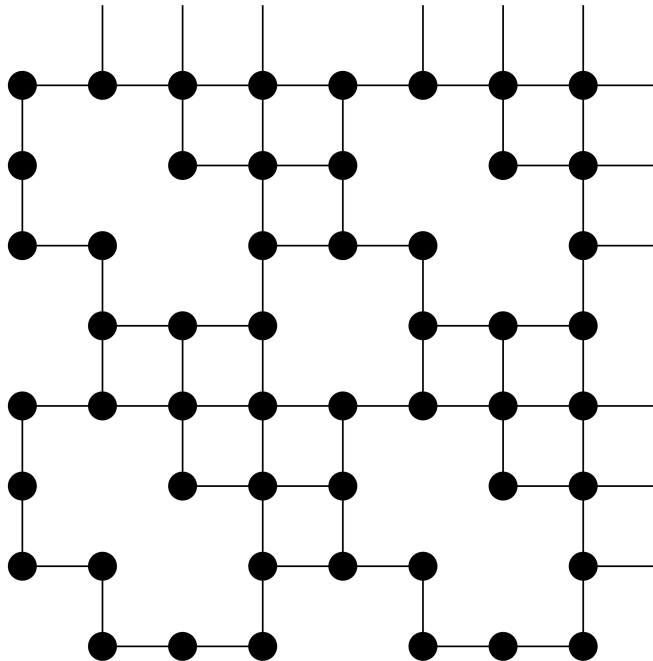
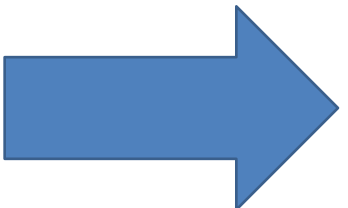
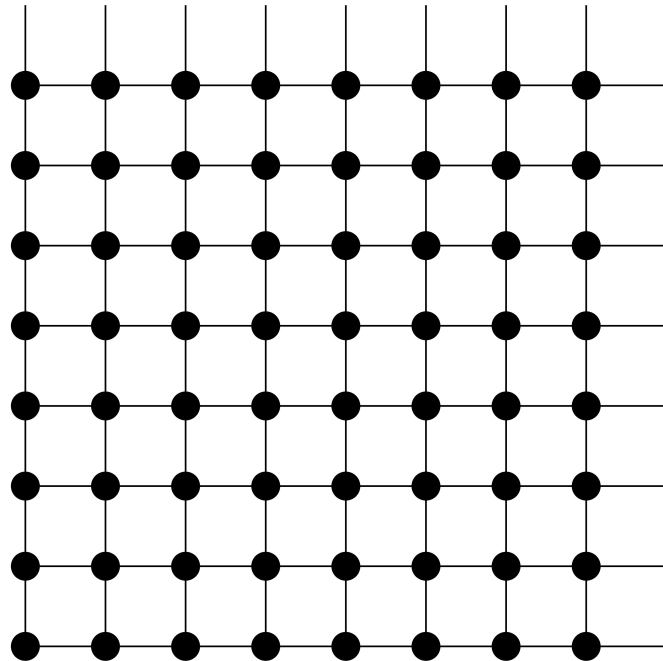


Fig. Initial enlarged square lattice

Fig. Periodic removal of sites

Vacancy engineering technique to create desired symmetries

- Our goal is to create the nonsymmorphic pattern in graphene
- We will do this by using vacancy engineering
- Instead of rebuilding the Hamiltonian each time, we project out the sites

$$H = t \sum_{\langle i,j \rangle \sigma} c_{i\sigma}^\dagger c_{j\sigma} + U \sum_{i \in \text{vac}\sigma} c_{i\sigma}^\dagger c_{i\sigma}$$

Vacancy engineering technique to create desired symmetries

- Our goal is to create the nonsymmorphic pattern in graphene
- We will do this by using vacancy engineering
- Instead of rebuilding the Hamiltonian each time, we project out the sites

$$H = t \sum_{\langle i,j \rangle \sigma} c_{i\sigma}^\dagger c_{j\sigma} + U \sum_{i \in \text{vac}\sigma} c_{i\sigma}^\dagger c_{i\sigma}$$


Vacancy engineering technique to create desired symmetries

- Our goal is to create the nonsymmorphic pattern in graphene
- We will do this by using vacancy engineering
- Instead of rebuilding the Hamiltonian each time, we project out the sites

$$H = t \sum_{\langle i,j \rangle \sigma} c_{i\sigma}^\dagger c_{j\sigma} + U \sum_{i \in \text{vac}\sigma} c_{i\sigma}^\dagger c_{i\sigma}$$

A blue arrow points from the term $U \sum_{i \in \text{vac}\sigma} c_{i\sigma}^\dagger c_{i\sigma}$ in the equation to the text "Very large" located below it.

Very large

Numerical results on engineered graphene

Notation: C_N

Number of sites in the vacancy
engineered unit-cell

Numerical results on engineered graphene

Notation: C_N

Number of sites in the vacancy
engineered unit-cell

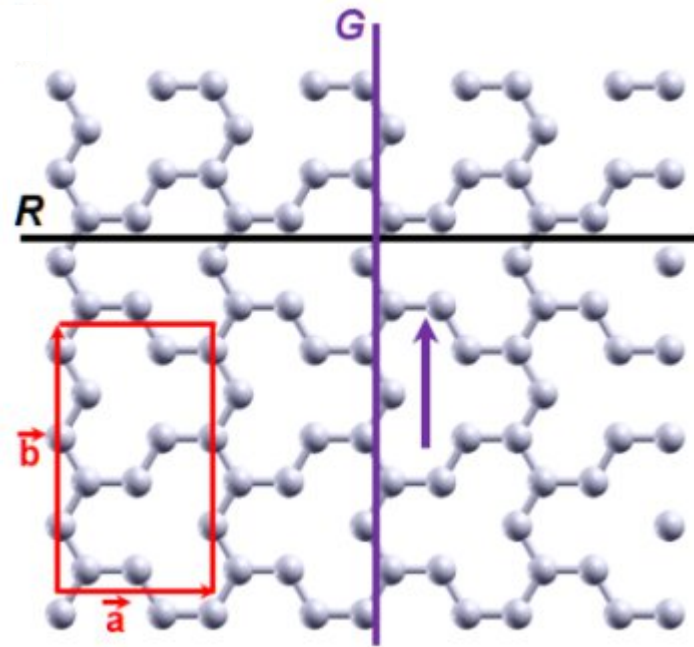


Fig. Unit-cell of vacancy
engineered C10

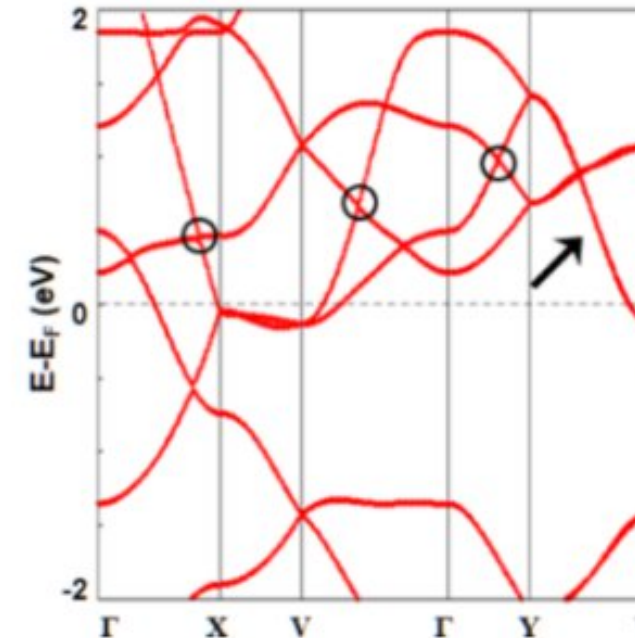


Fig. Bandstructure of C10
showing nodal lines along Y-V

Numerical results on engineered graphene

Notation: C_N

Number of sites in the vacancy
engineered unit-cell

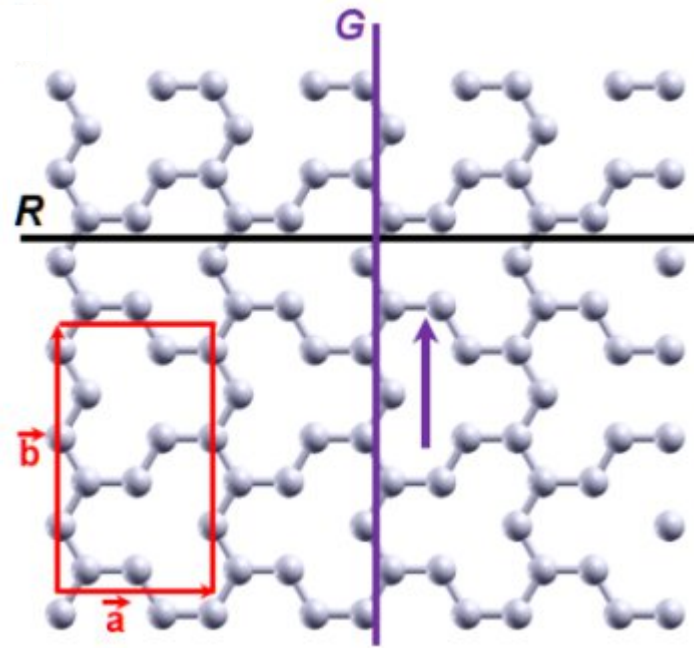


Fig. Unit-cell of vacancy
engineered C10

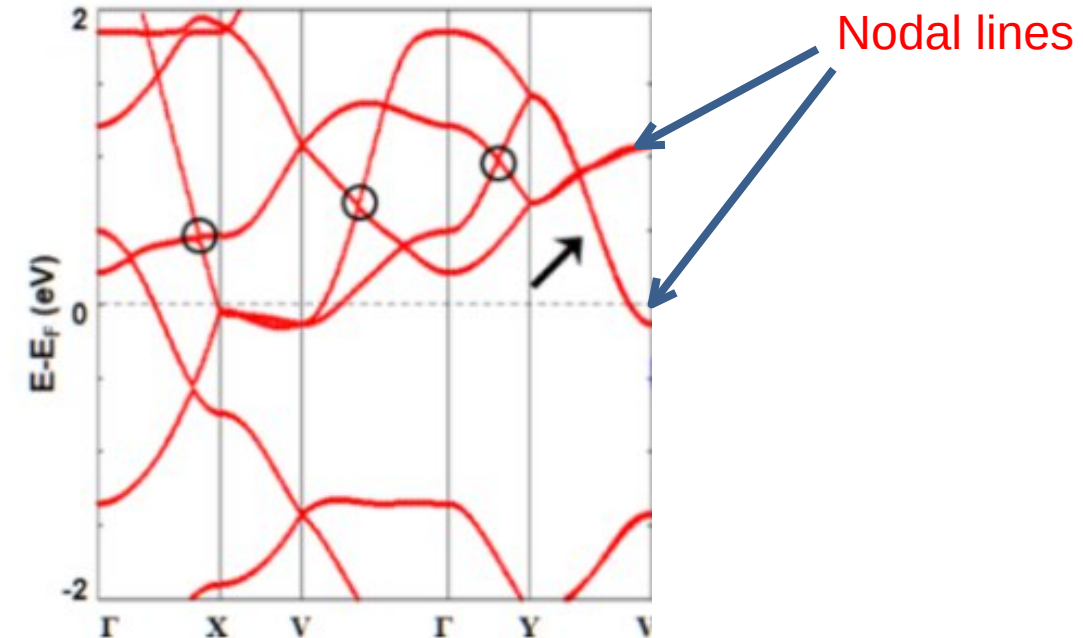


Fig. Bandstructure of C10
showing nodal lines along Y-V

Numerical results on engineered graphene

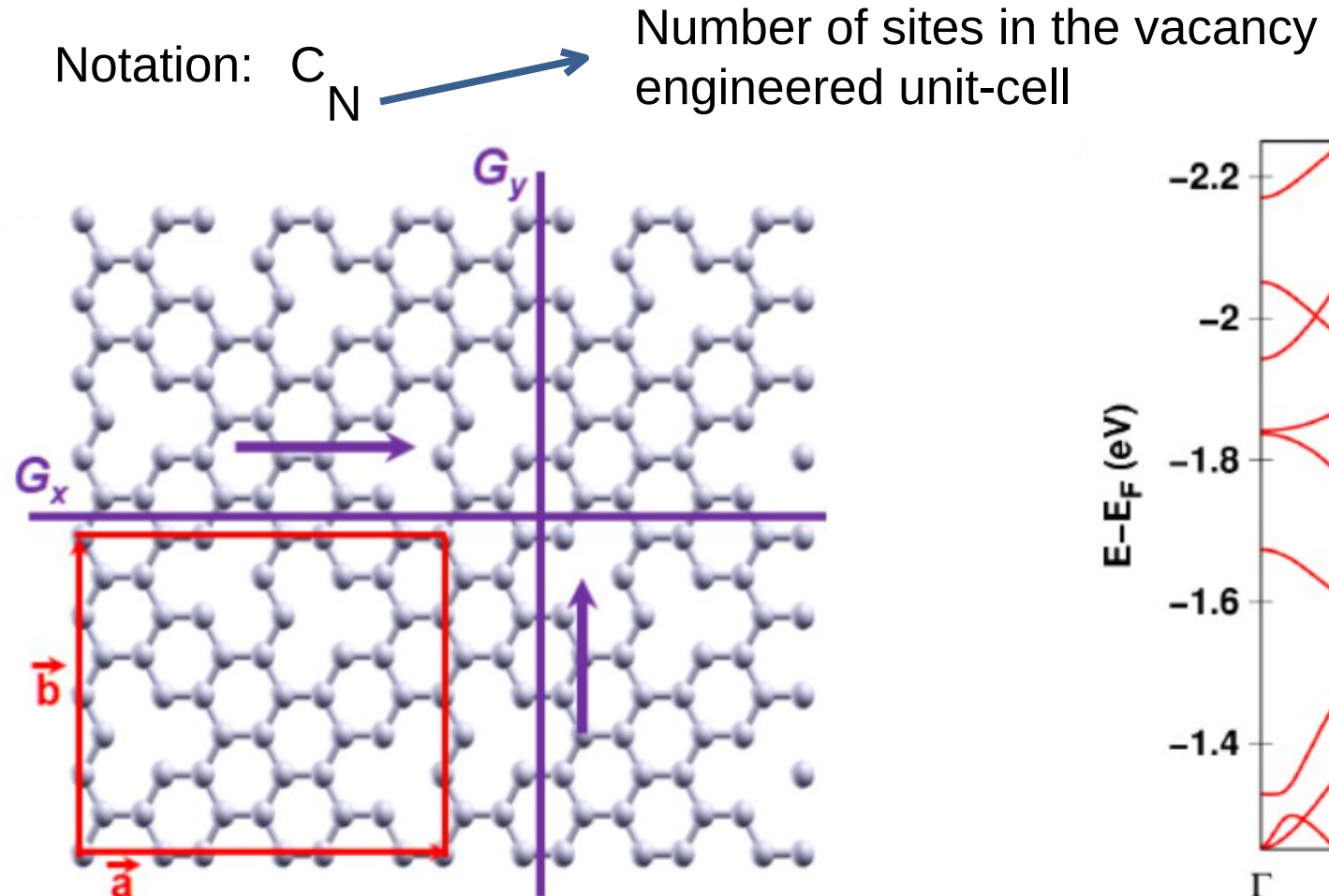


Fig. Unit-cell of vacancy engineered C44

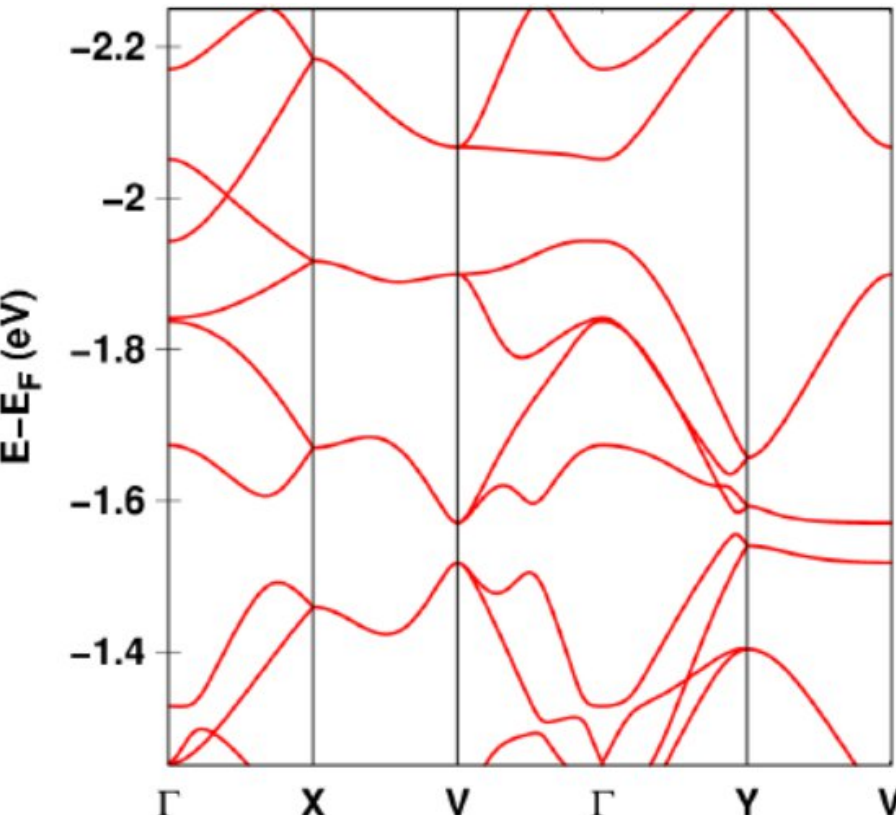


Fig. Bandstructure of C44 showing nodal loops

Numerical results on engineered graphene

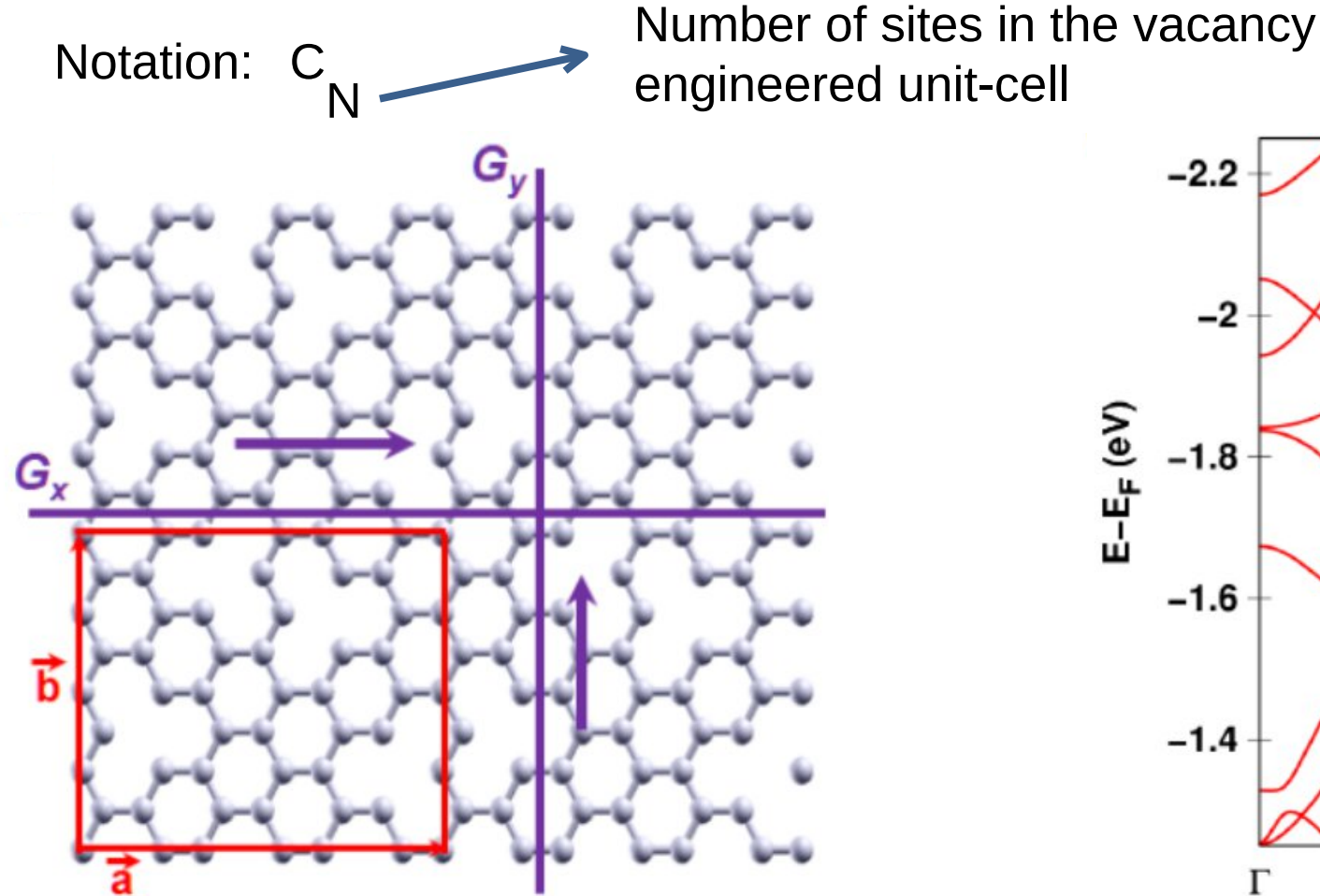


Fig. Unit-cell of vacancy engineered C44

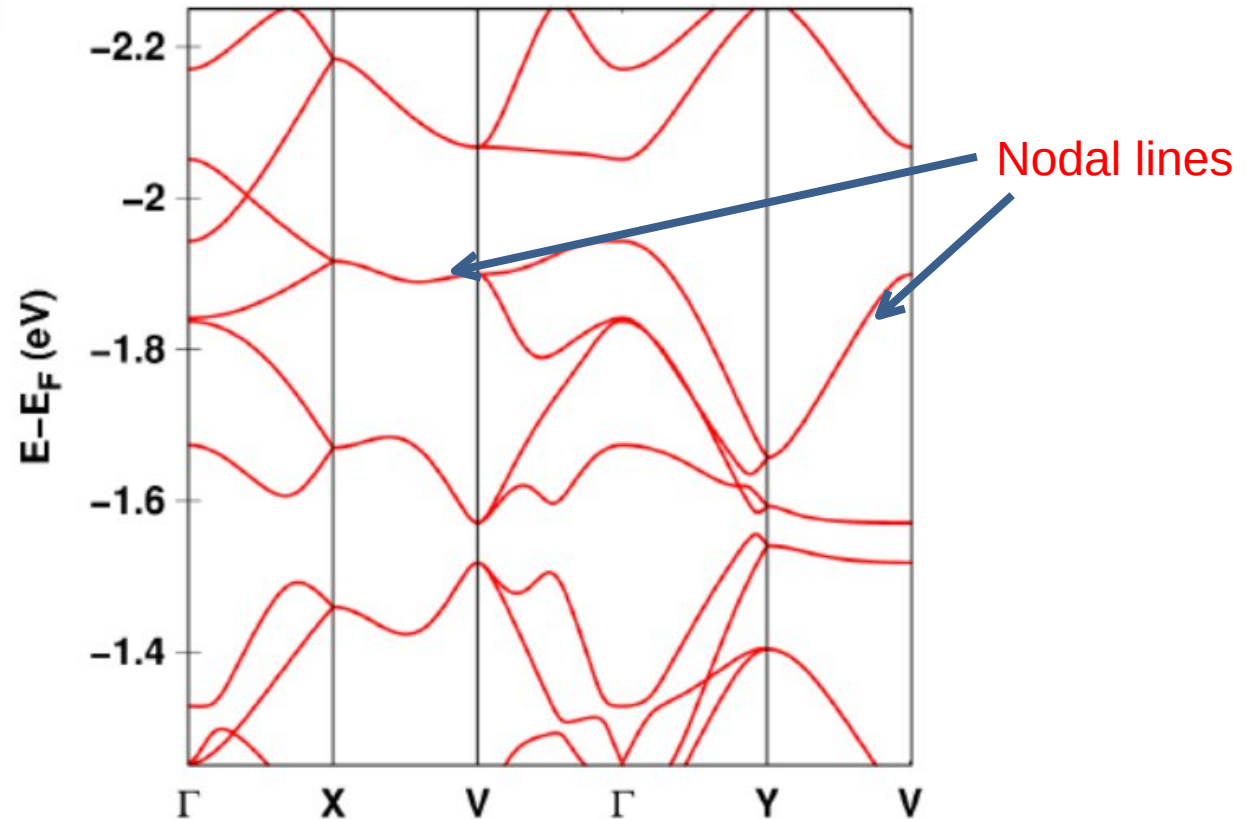


Fig. Bandstructure of C44 showing nodal loops

Connection to experiments on nanoporous graphene

- There are several experimental techniques to create “holey materials”, such as graphene [1].
- In fact, these nodal lines have already been observed experimentally [2].

[1] de Sousa, M. S., Liu, F., Malard, M., Qu, F., & Chen, W. (2022). *Physical Review B*, 105(15), 155414.

[2] Jacobse, P. H. et al. *J. Am. Chem. Soc.* 142, 13507–13514 (2020).

Connection to experiments on nanoporous graphene

- There are several experimental techniques to create “holey materials”, such as graphene [1].
- In fact, these nodal lines have already been observed experimentally [2].

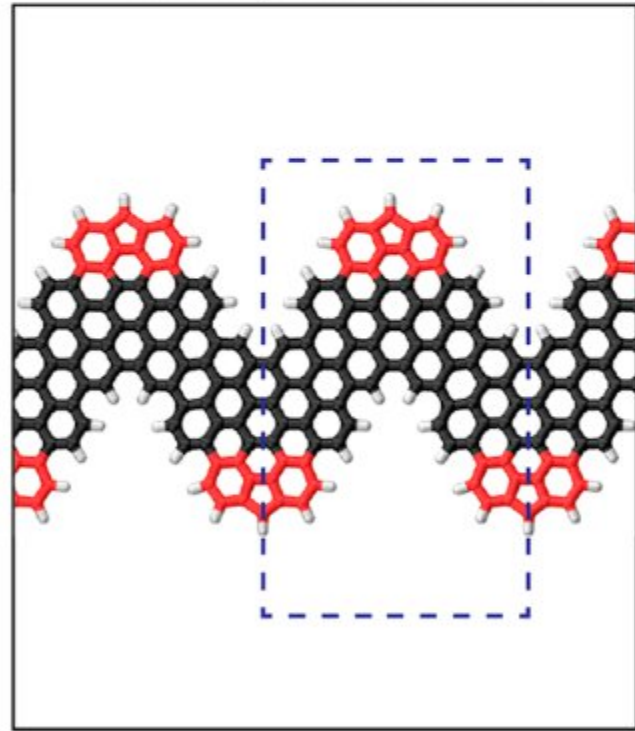


Fig. fluorenyl-chevron graphene nanoribbon [2].

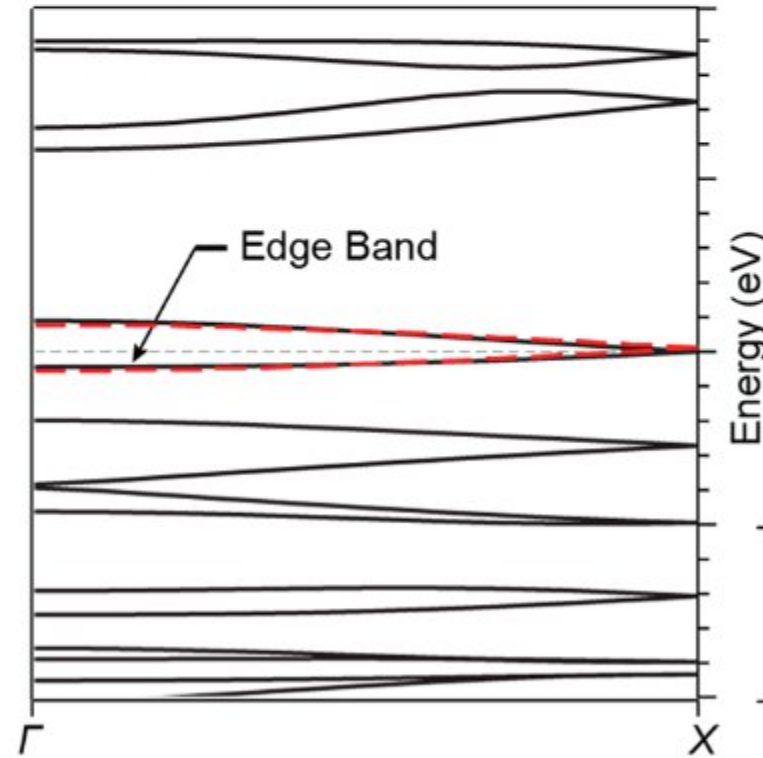


Fig. Band structure showing every two bands sticking together [2].

- [1] de Sousa, M. S., Liu, F., Malard, M., Qu, F., & Chen, W. (2022). *Physical Review B*, 105(15), 155414.
[2] Jacobse, P. H. et al. *J. Am. Chem. Soc.* 142, 13507–13514 (2020).

Connection to experiments on nanoporous graphene

- There are several experimental techniques to create “holey materials”, such as graphene [1].
- In fact, these nodal lines have already been observed experimentally [2].

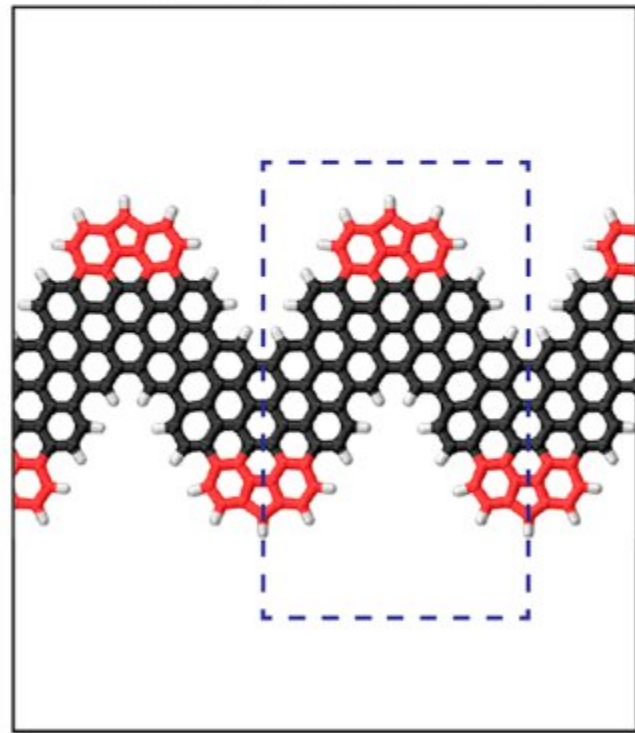


Fig. fluorenyl-chevron graphene nanoribbon [2].

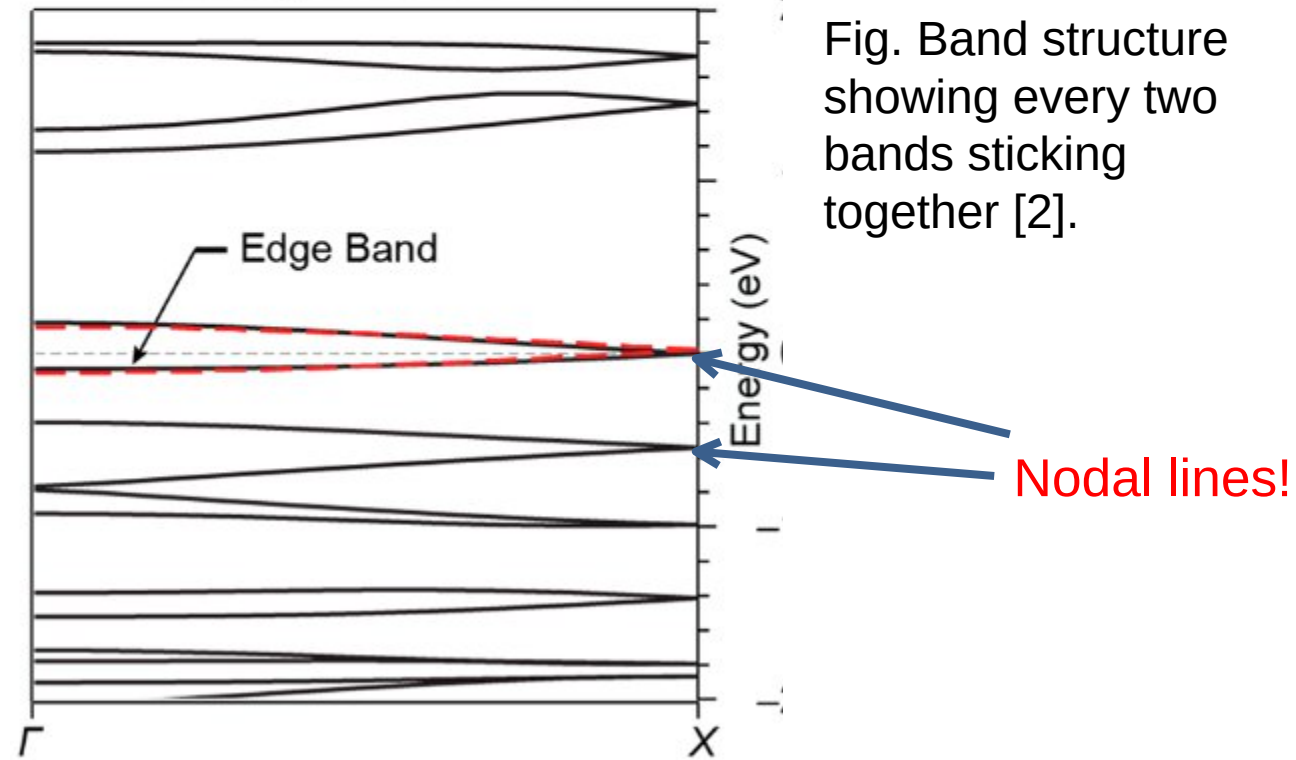


Fig. Band structure showing every two bands sticking together [2].

- [1] de Sousa, M. S., Liu, F., Malard, M., Qu, F., & Chen, W. (2022). *Physical Review B*, 105(15), 155414.
[2] Jacobse, P. H. et al. *J. Am. Chem. Soc.* 142, 13507–13514 (2020).

Robustness of nodal lines to perturbations that preserve symmetry

- We show that the nodal lines are actually robust to RSOC
- The spin degeneracy is lifted, but there is still nodal lines

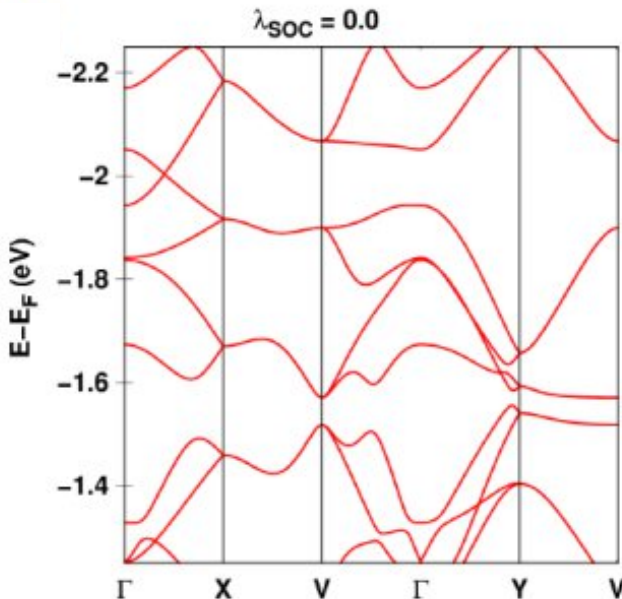


Fig.
Bandstructure of
C44 without
RSOC

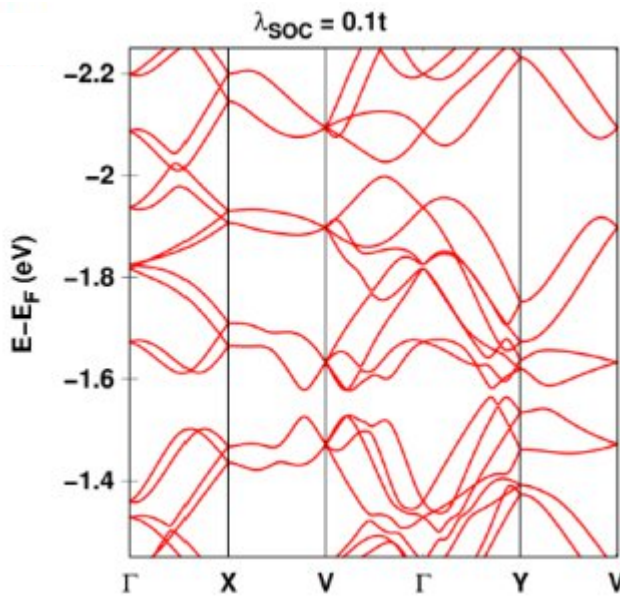


Fig. C44 with
RSOC still nodal
loops
but lifted spin
degeneracy

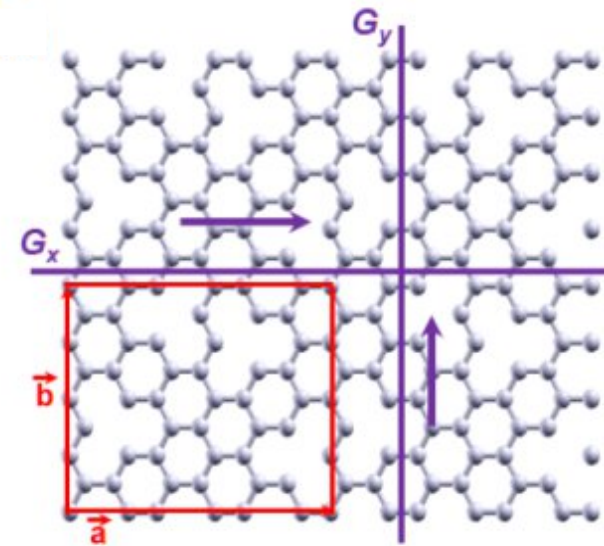


Fig. Unit-cell
of C44

Introduction to bipartite lattices and zero modes

- We wanted to investigate zero-energy flat-bands (ZEFBs) in graphene, similar to [1].
- With ZEFBs, the DOS will be enlarged at the Fermi level, interesting electronic phenomena.
- We show that we can use vacancy engineering to create flat-bands generically.

Introduction to bipartite lattices and zero modes

- We wanted to investigate zero-energy flat-bands (ZEFBs) in graphene, similar to [1].
- With ZEFBs, the DOS will be enlarged at the Fermi level, interesting electronic phenomena.
- We show that we can use vacancy engineering to create flat-bands generically.

Fig. Lead apatite,
“LK-99” [2].

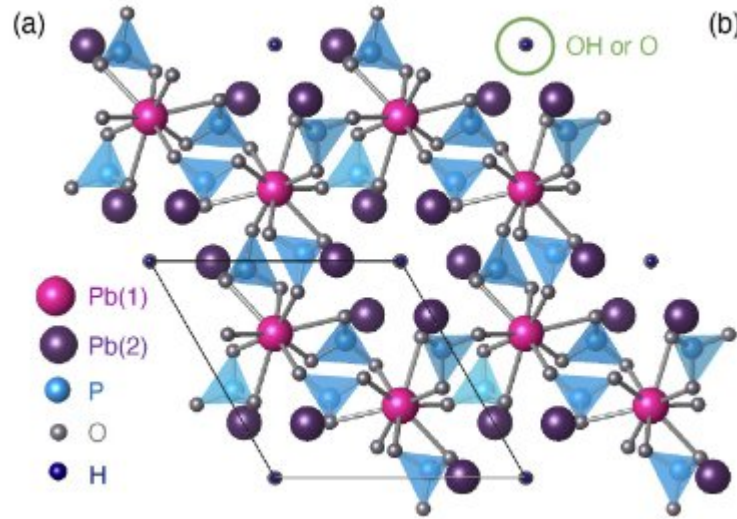
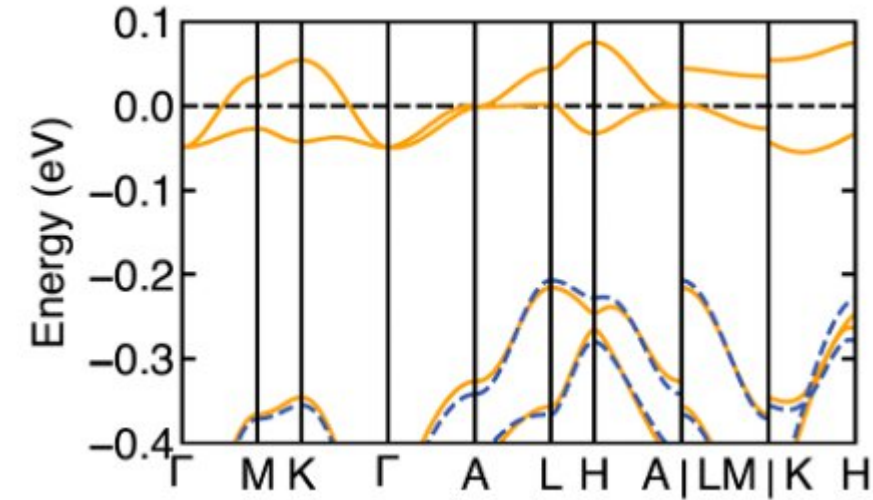


Fig. Spin-polarized electronic band structure showing narrow bands [2].



[1] Lieb, E. H. (1989). Physical review letters, 62(10), 1201.

[2] Griffin, S. M. (2023). *arXiv:2307.16892*.

[3] Lee, S., Kim, J., Kim, H. T., Im, S., An, S., & Auh, K. H. (2023). *arXiv:2307.12037*.

Introduction to bipartite lattices and zero modes

- We wanted to investigate zero-energy flat-bands (ZEFBs) in graphene, similar to [1].
- With ZEFBs, the DOS will be enlarged at the Fermi level, interesting electronic phenomena.
- We show that we can use vacancy engineering to create flat-bands generically.

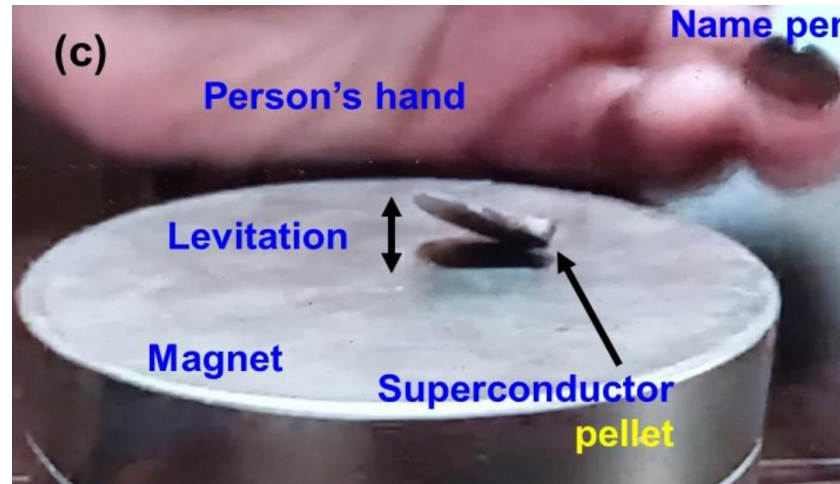


Fig. (Maybe?) A room-temperature superconductor [3].

[1] Lieb, E. H. (1989). Physical review letters, 62(10), 1201.

[2] Griffin, S. M. (2023). *arXiv:2307.16892*.

[3] Lee, S., Kim, J., Kim, H. T., Im, S., An, S., & Auh, K. H. (2023). *arXiv:2307.12037*.

Creating flat-band with periodic vacancies

- Lieb showed [1] that for a bipartite lattice, we can have flat-bands if there is unbalance.
- We analyze the problem using the rank-nullity theorem.

[1] Lieb, E. H. (1989). Physical review letters, 62(10), 1201.

Creating flat-band with periodic vacancies

- Lieb showed [1] that for a bipartite lattice, we can have flat-bands if there is unbalance.
- We analyze the problem using the rank-nullity theorem.

$$r(H) + \eta(H) = \dim(H),$$

Rank Nullity Dimension

[1] Lieb, E. H. (1989). Physical review letters, 62(10), 1201.

Rank-nullity theorem argument for emergence of flat bands

- Lieb showed [1] that for a bipartite lattice, we can have flat-bands if there is unbalance.
- We analyze the problem using the rank-nullity theorem.
- In the case of bipartite lattice, it takes a simple form:

$$H(\mathbf{k}) = \begin{pmatrix} & & | & Q(\mathbf{k}) \\ & & | & \\ \hline & & | & \\ Q^\dagger(\mathbf{k}) & & | & \end{pmatrix}$$

$$\begin{aligned} r(H) + \eta(H) &= \dim(H), \\ r(Q) + \eta(Q) &= \dim(Q), \\ r(Q^\dagger) + \eta(Q^\dagger) &= \dim(Q^\dagger). \end{aligned}$$

Eq. The Hamiltonian of bipartite lattice
is anti-block-diagonal

[1] Lieb, E. H. (1989). Physical review letters, 62(10), 1201.

Rank-nullity theorem argument for emergence of flat bands

- Lieb showed [1] that for a bipartite lattice, we can have flat-bands if there is unbalance.
- We analyze the problem using the rank-nullity theorem.
- In the case of bipartite lattice, it takes a simple form:

$$H(\mathbf{k}) = \begin{pmatrix} & & | & Q(\mathbf{k}) \\ & & | & \\ \hline & & | & \\ Q^\dagger(\mathbf{k}) & & | & \end{pmatrix}$$

Eq. The Hamiltonian of bipartite lattice
is anti-block-diagonal

- We recover the Lieb theorem

$$\eta(H) = N_B - N_A + 2\eta(Q)$$

- The wave-function is localized at the majority sublattice

[1] Lieb, E. H. (1989). Physical review letters, 62(10), 1201.

Vacancy-engineering for creating flat-bands

- Vacancy engineering let us create flat-bands generically
- Consider constructing the Lieb lattice:

$$H(\mathbf{k}) = \begin{pmatrix} 0 & 0 & te^{ik_x} & te^{-ik_y} \\ 0 & 0 & te^{-ik_y} & te^{ik_x} \\ te^{-ik_x} & te^{ik_y} & 0 & 0 \\ te^{ik_y} & te^{-ik_x} & 0 & 0 \end{pmatrix}$$

Fig. Square
lattice model

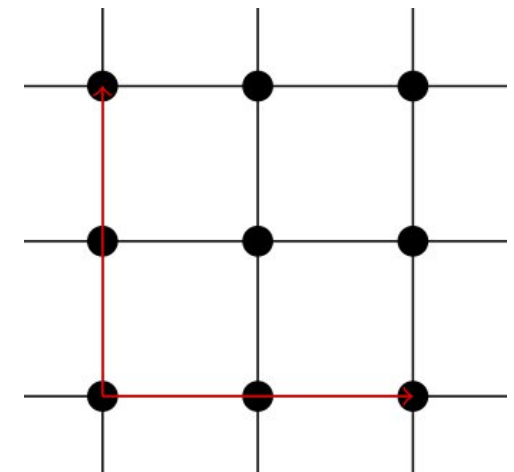
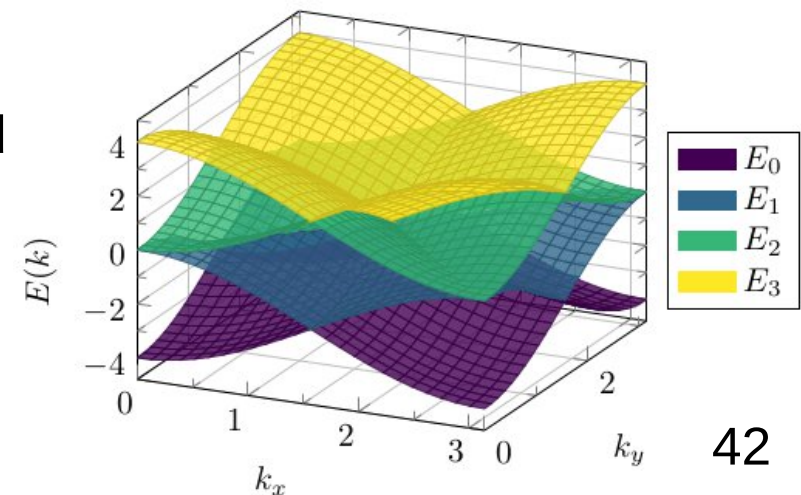


Fig. Band
structure



Vacancy-engineering for creating flat-bands

- Vacancy engineering let us create flat-bands generically
- Consider constructing the Lieb lattice:

$$H(\mathbf{k}) = \begin{pmatrix} 0 & 0 & te^{ik_x} & te^{-ik_y} \\ 0 & 0 & te^{-ik_y} & te^{ik_x} \\ te^{-ik_x} & te^{ik_y} & 0 & 0 \\ te^{ik_y} & te^{-ik_x} & 0 & 0 \end{pmatrix}$$

$N_A = N_B$

Fig. Square lattice model

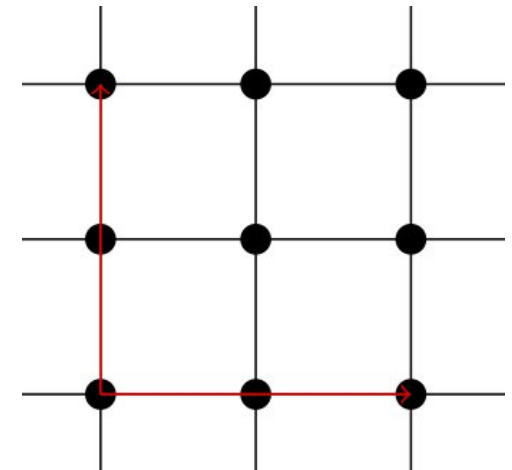
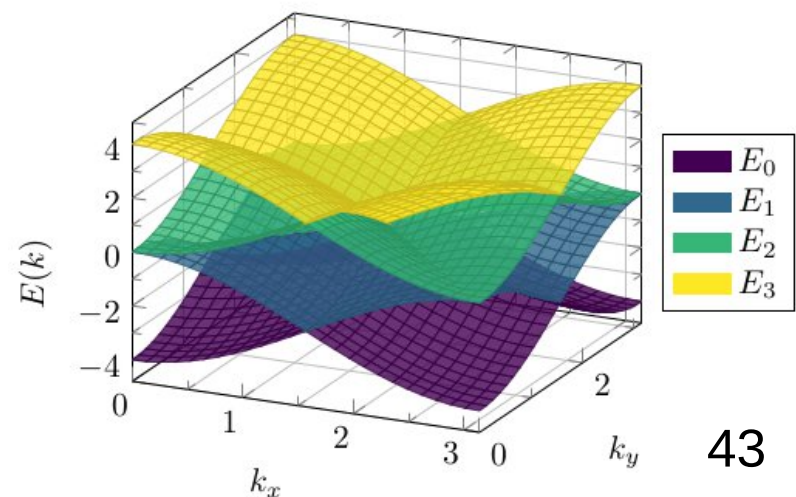


Fig. Band structure



Vacancy-engineering for creating flat-bands

- Vacancy engineering let us create flat-bands generically
- Consider constructing the Lieb lattice:

$$H(\mathbf{k}) = \begin{pmatrix} 0 & 0 & te^{ik_x} & \\ 0 & 0 & te^{-ik_y} & \\ te^{-ik_x} & te^{ik_y} & 0 & \\ & & & \end{pmatrix}$$

Fig. Square
lattice model

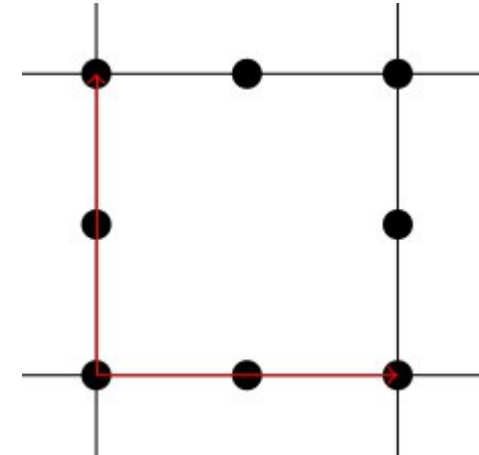
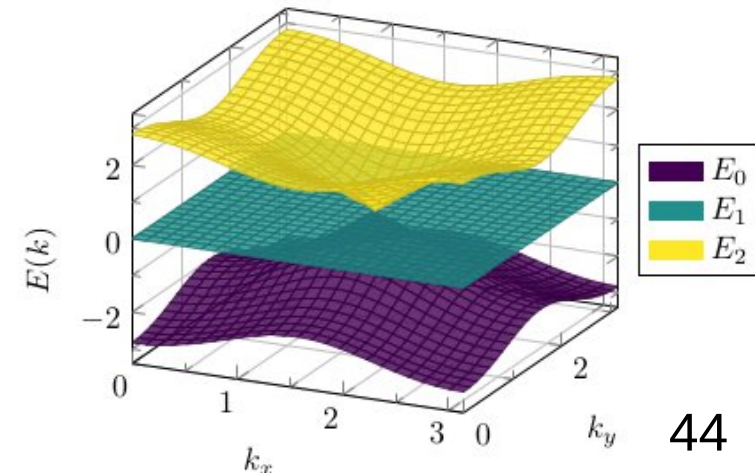


Fig. Band
structure



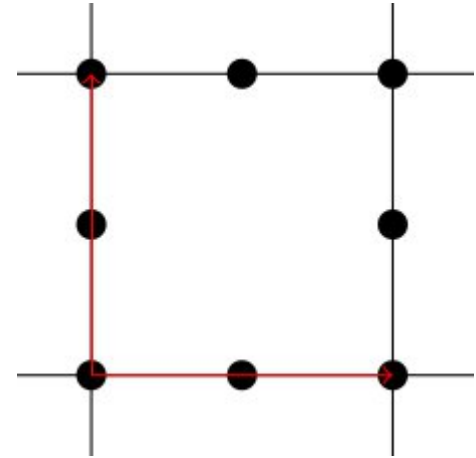
Vacancy-engineering for creating flat-bands

- Vacancy engineering let us create flat-bands generically
- Consider constructing the Lieb lattice:

$$H(\mathbf{k}) = \begin{pmatrix} 0 & 0 & te^{ik_x} & 0 \\ 0 & 0 & te^{-ik_y} & 0 \\ te^{-ik_x} & te^{ik_y} & 0 & 0 \\ 0 & 0 & 0 & 0 \end{pmatrix}$$

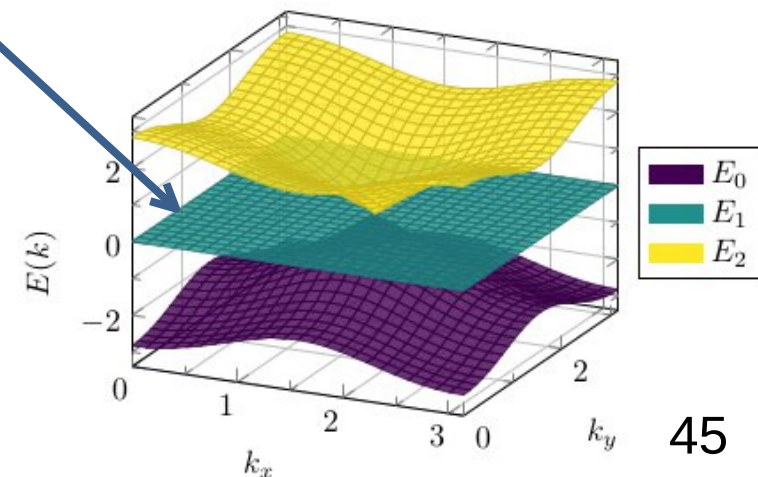
$N_A \neq N_B$

Fig. Square lattice model



Flat-band at zero energy

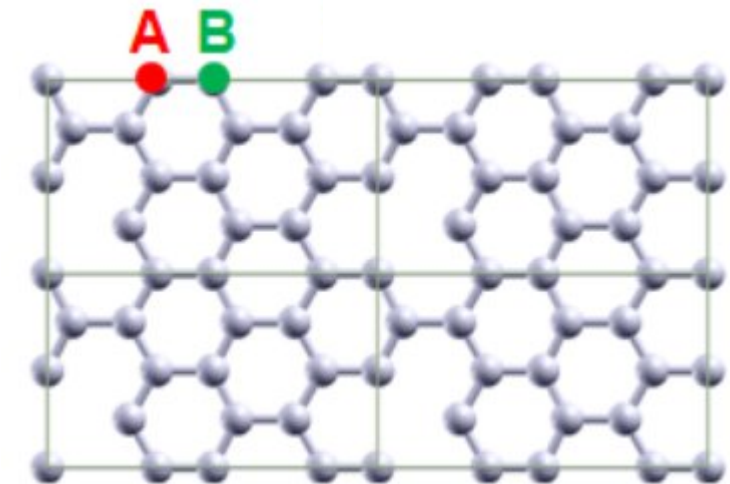
Fig. Band structure



Tight-binding model results

- We investigate the case with chiral symmetry

Fig. Unit-cell
of vacancy
engineered
graphene
C15



Tight-binding model results

- We investigate the case with chiral symmetry

Fig. C15 band structure showing perfect flat-bands

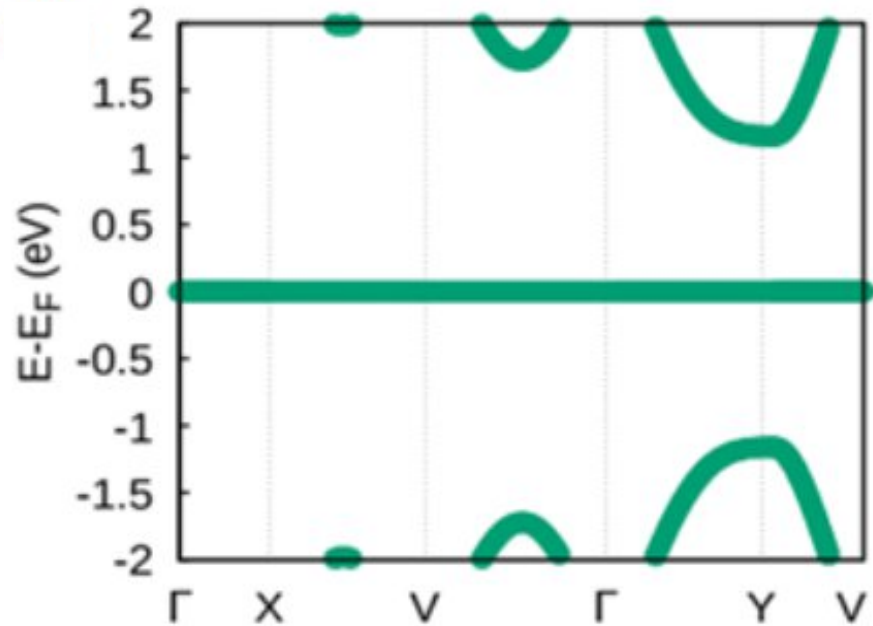


Fig. Unit-cell of vacancy engineered graphene C15

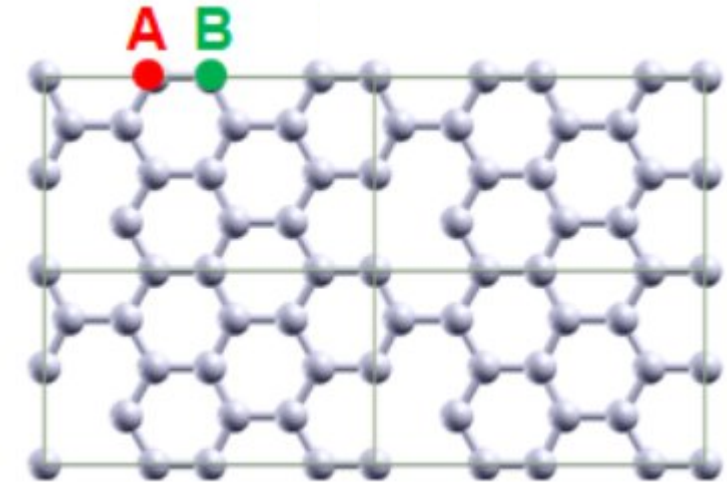
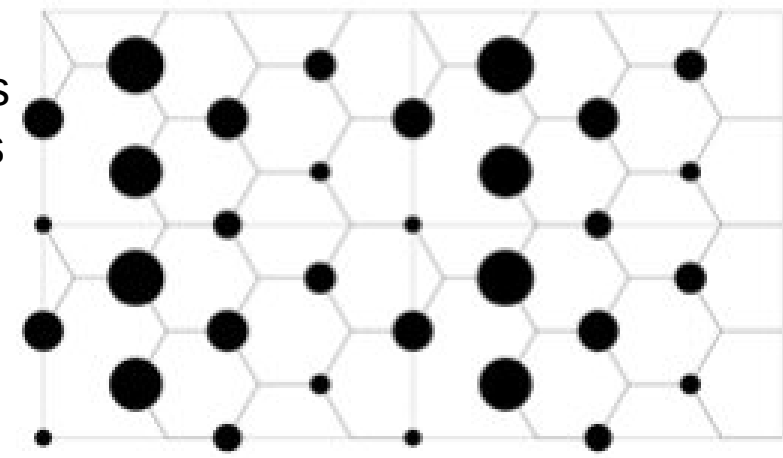


Fig. Wave-function weights at different sites



Tight-binding model results

- We investigate the case with chiral symmetry
- And a more realistic model without it

Fig. C15 band structure showing narrow bands

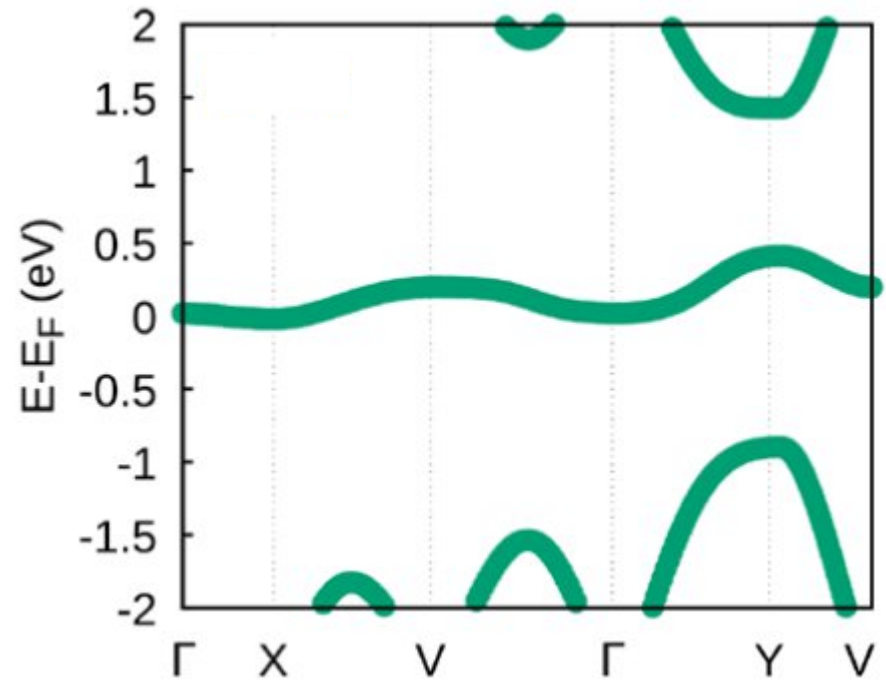


Fig. Unit-cell of vacancy engineered graphene C15

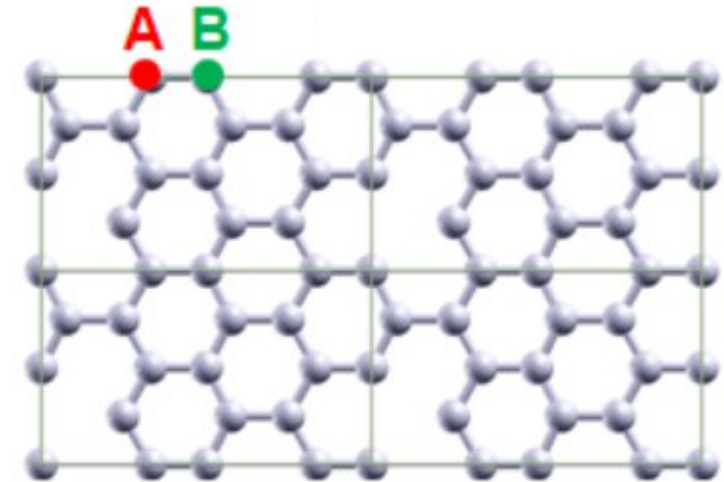
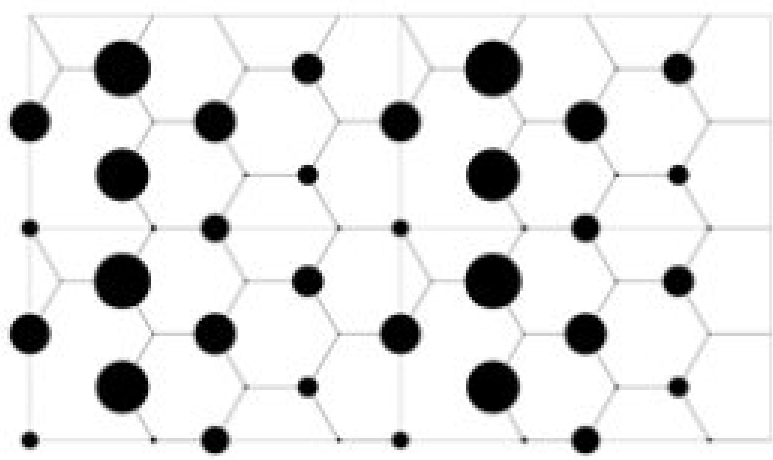


Fig. Wave-function weights at different sites



Tight-binding model results

- We investigate the case with chiral symmetry
- And a more realistic model without it

Fig. C15 band structure showing narrow bands

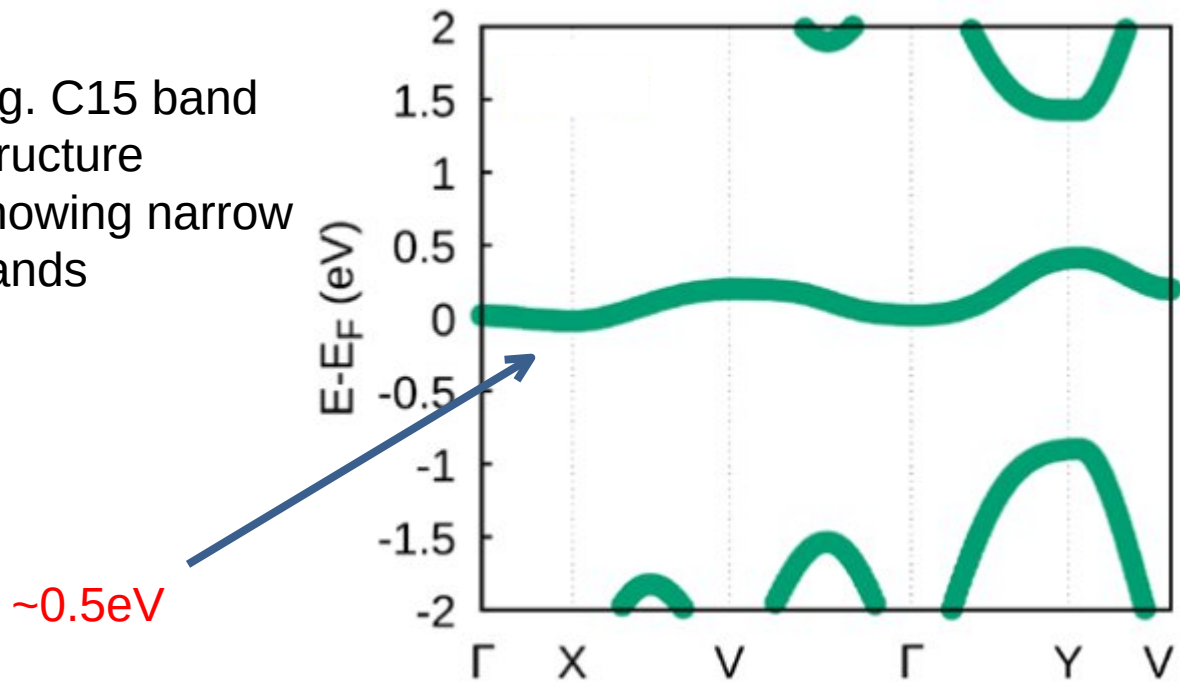


Fig. Unit-cell of vacancy engineered graphene C15

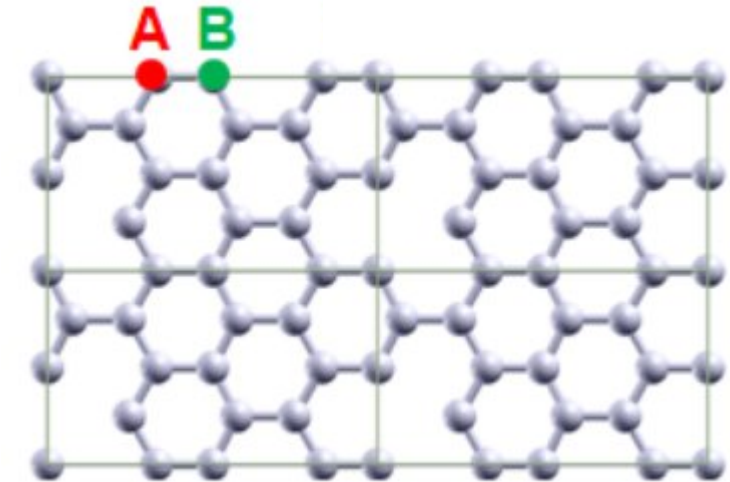
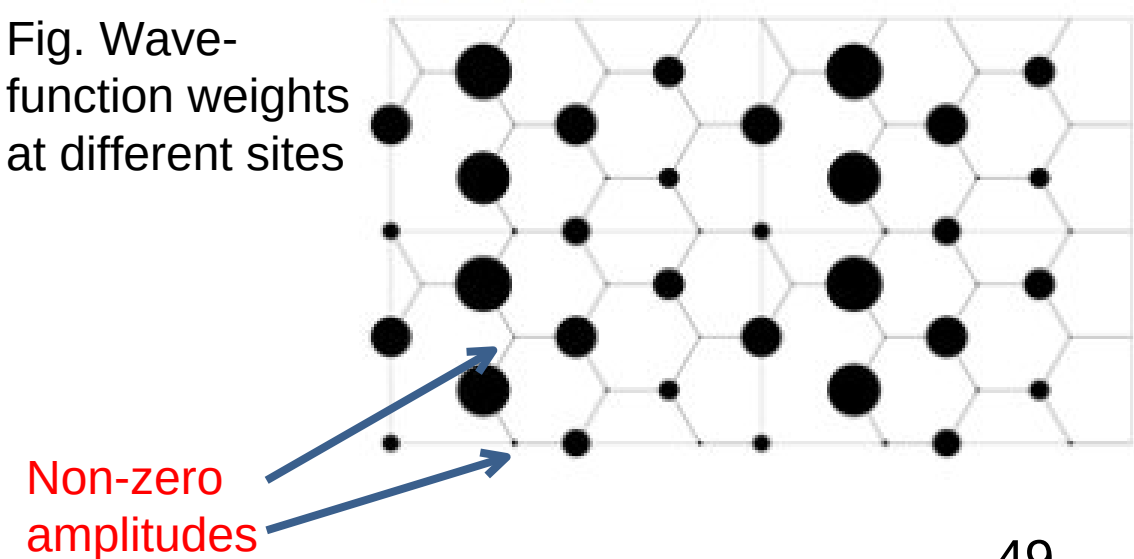


Fig. Wave-function weights at different sites



Investigating s-wave Superconductivity in Flat Bands

- Intrigued by the enlarged DOS of narrows bands [1,2], we investigate superconductivity.
- We use Bogoliubov-de Gennes weak coupling mean field [3], solving it self-consistently.

$$\begin{aligned} H = & \sum_{\langle ij \rangle \sigma} t c_{i\sigma}^\dagger c_{j\sigma} + \sum_{\langle\langle ij \rangle\rangle \sigma} t' c_{i\sigma}^\dagger c_{j\sigma} - \sum_{i\sigma} \mu c_{i\sigma}^\dagger c_{i\sigma} \\ & + \sum_i (\Delta_i c_{i\uparrow}^\dagger c_{i\downarrow}^\dagger + \Delta_i^* c_{i\downarrow} c_{i\uparrow}) + U \sum_{i \in v} c_{i\sigma}^\dagger c_{i\sigma}, \end{aligned}$$

- Self-consistent condition

$$\Delta_i = \sum_{\mathbf{k}} V \theta(\omega_D - E_{\mathbf{k}}) [2f(E_{\mathbf{k}}) - 1] u_{\mathbf{k}}(i) v_{\mathbf{k}}^*(i)$$

[1] Roy, B., & Juričić, V. (2019). *Physical Review B*, 99(12), 121407.

[2] Morell, E. S., Correa, J. D., Vargas, P., Pacheco, M., & Barticevic, Z. (2010). *Physical Review B*, 82(12), 121407. 50

[3] de Gennes, P. G. (1989). *Superconductivity of Metals and Alloys*.

Numerical results

Fig. Pairing amplitudes for C15

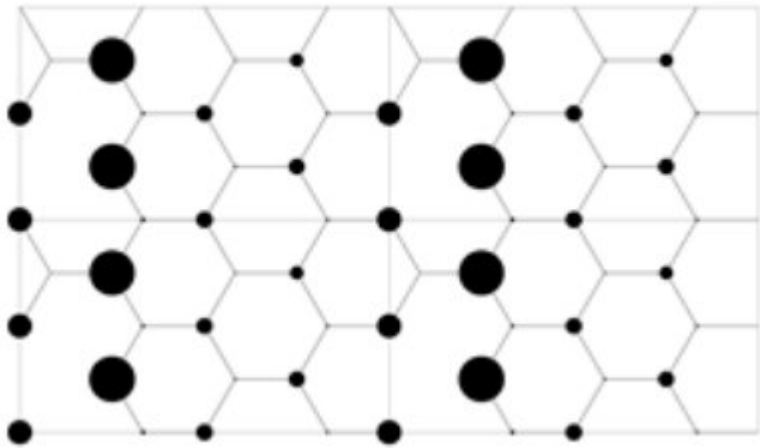


Fig. Pairing potential dependence at T=0

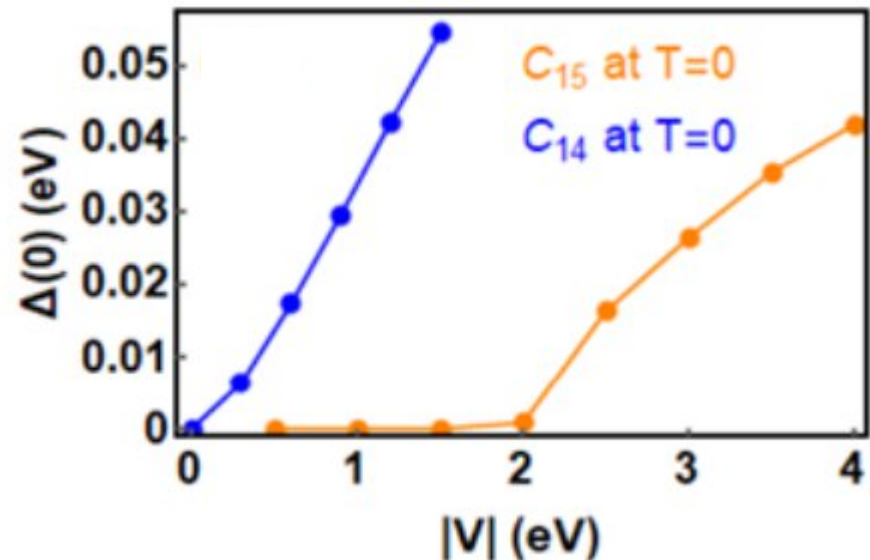


Fig. Unit-cell of vacancy engineered graphene C15

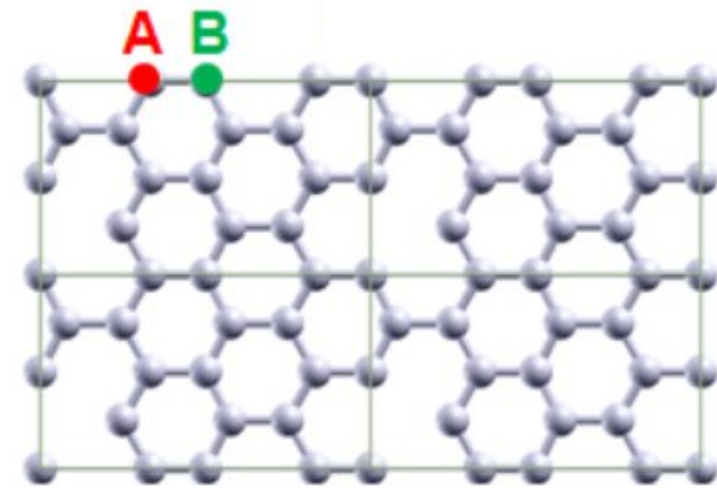
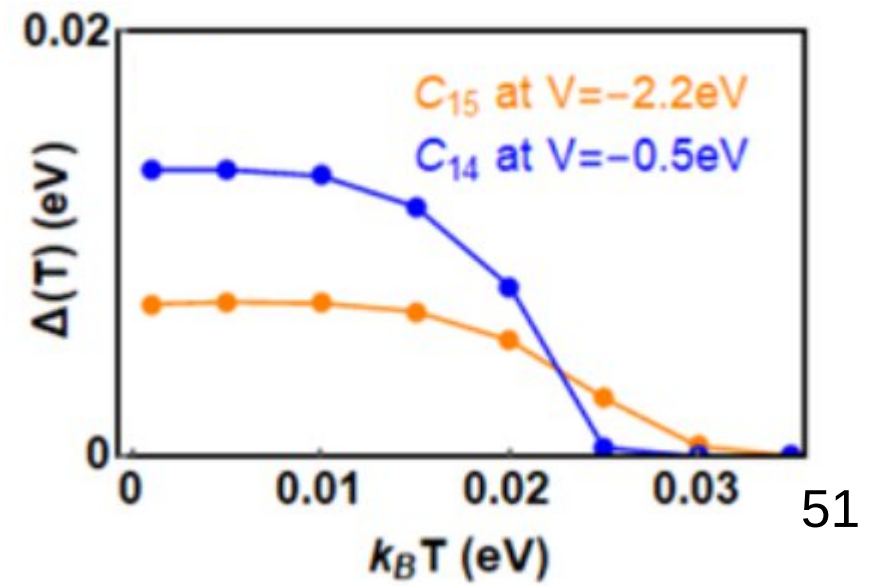


Fig. Temperature dependence



Numerical results

Fig. Pairing amplitudes for C14

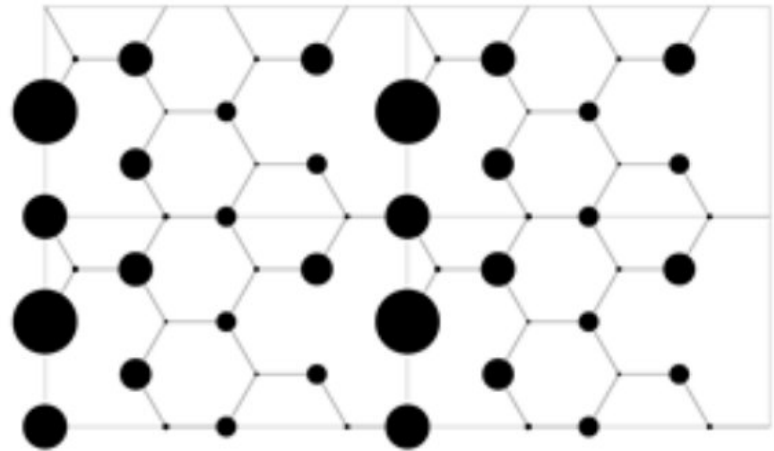


Fig. Pairing potential dependence at T=0

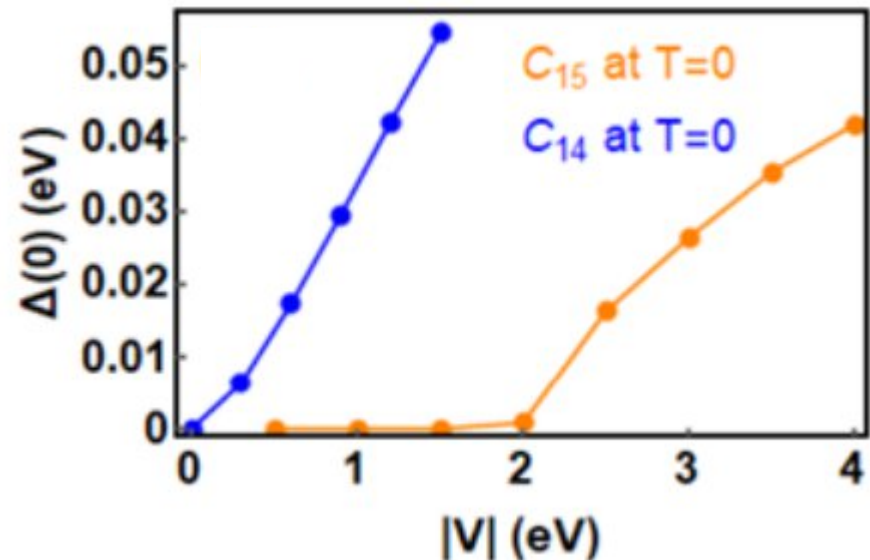


Fig. Unit-cell of vacancy engineered graphene C14

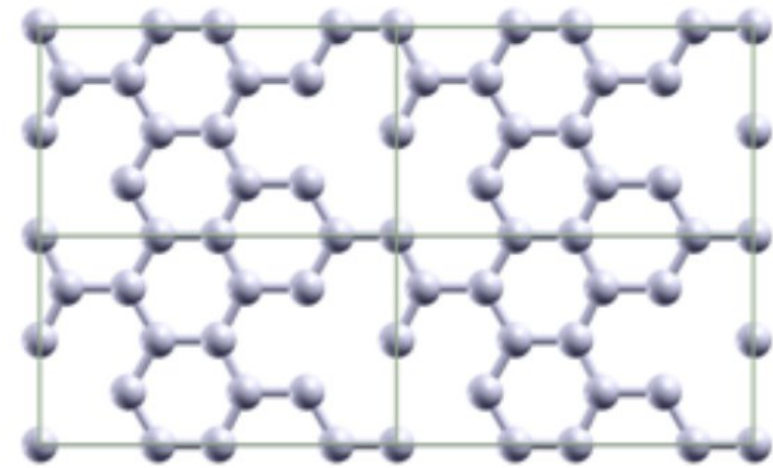
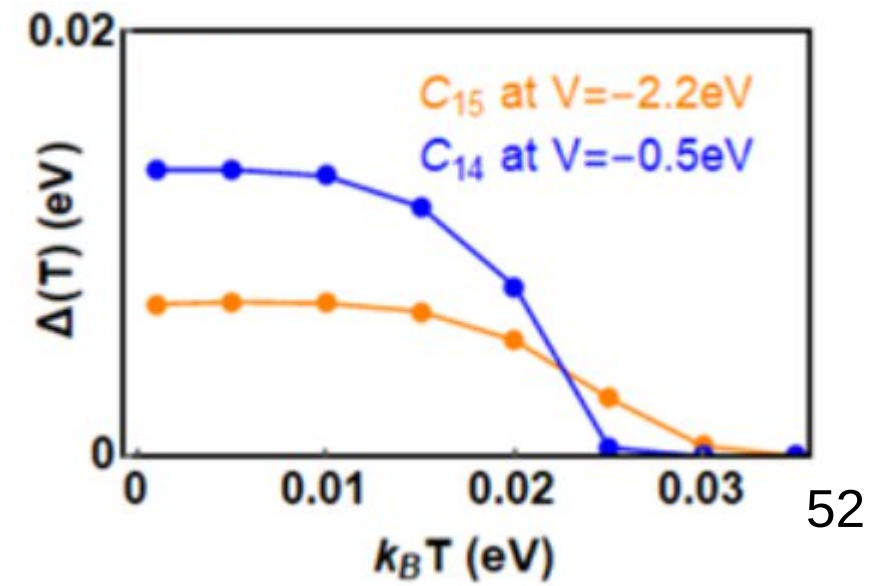


Fig. Temperature dependence



Quantum metric and fidelity number

We start with the fully anti-symmetric valance state of gapped material

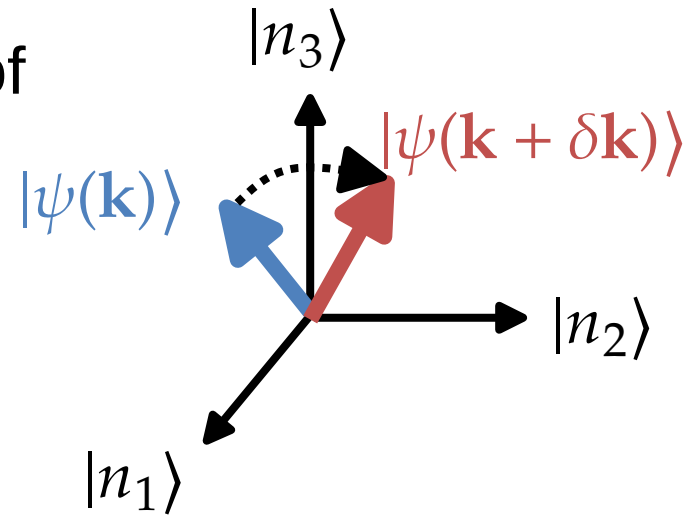
$$|u^{val}(\mathbf{k})\rangle = \frac{1}{\sqrt{N_-}} \epsilon^{n_1 n_2 \dots n_{N_-}} |n_1(\mathbf{k})\rangle |n_2(\mathbf{k})\rangle \dots |n_{N_-}(\mathbf{k})\rangle$$

The quantum metric is defined as

$$|\langle u(\mathbf{k})|u(\mathbf{k} + d\mathbf{k})\rangle| = 1 - \frac{1}{2} g_{\mu\nu} dk^\mu dk^\nu$$

It can be shown to be

$$g_{\mu\nu}(\mathbf{k}) = \frac{1}{2} \sum_{nm} \langle \partial_\mu n | m \rangle \langle m | \partial_\nu n \rangle + \langle \partial_\nu n | m \rangle \langle m | \partial_\mu n \rangle$$



[1] Provost, J. P., Vallee, G. (1980). *Communications in Mathematical Physics*, 76, 289-301.

[2] Marzari, N., & Vanderbilt, D. (1997). *Physical review B*, 56(20), 12847.

[3] Souza, I., Wilkens, T., & Martin, R. M. (2000). *Physical Review B*, 62(3), 1666.

Quantum metric and fidelity number

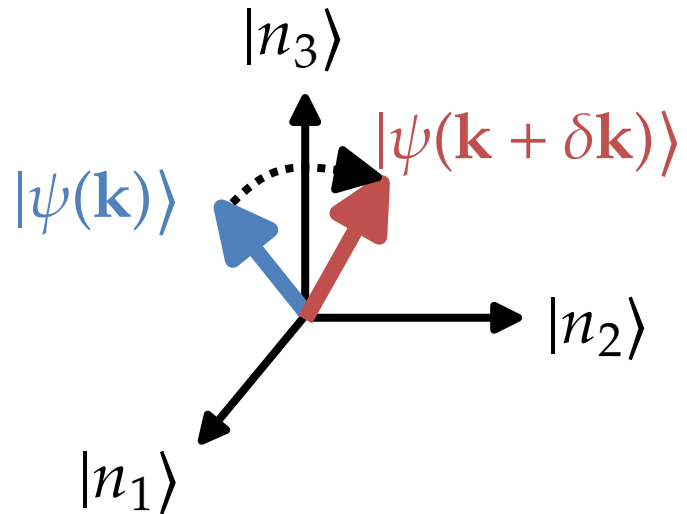
The integration of quantum metric over the BZ is

$$G_{\mu\nu}(\mathbf{k}) = \int \frac{d^D \mathbf{k}}{(2\pi)^2} g_{\mu\nu}(\mathbf{k}) \quad = \text{"fidelity number"}$$

which is related to the spread of the Wannier functions [2,3].

And the fidelity number spectral function

$$G_{\mu\nu}(\omega) = \int \frac{d^D \mathbf{k}}{(2\pi)^D} g_{\mu\nu}(\mathbf{k}, \omega) \quad G_{\mu\nu} = \int d\omega G_{\mu\nu}(\omega)$$



[1] Provost, J. P., Vallee, G. (1980). *Communications in Mathematical Physics*, 76, 289-301.

[2] Marzari, N., & Vanderbilt, D. (1997). *Physical review B*, 56(20), 12847.

[3] Souza, I., Wilkens, T., & Martin, R. M. (2000). *Physical Review B*, 62(3), 1666.

Quantum metric and fidelity number

Fidelity number spectral function:

$$G_{\mu\nu}(\omega) = \int \frac{d^D \mathbf{k}}{(2\pi)^D} g_{\mu\nu}(\mathbf{k}, \omega)$$

Since

$$\sigma_{\mu\mu}(\omega) = \frac{\pi e^2}{\hbar^{D-1}} \omega G_{\mu\mu}^d(\omega)$$

The optical absorption per unit-cell is

$$W_a(\omega) = \frac{\pi e^2}{2\hbar^{D-1}} E_0^2 \omega G_{\mu\mu}^d(\omega)$$

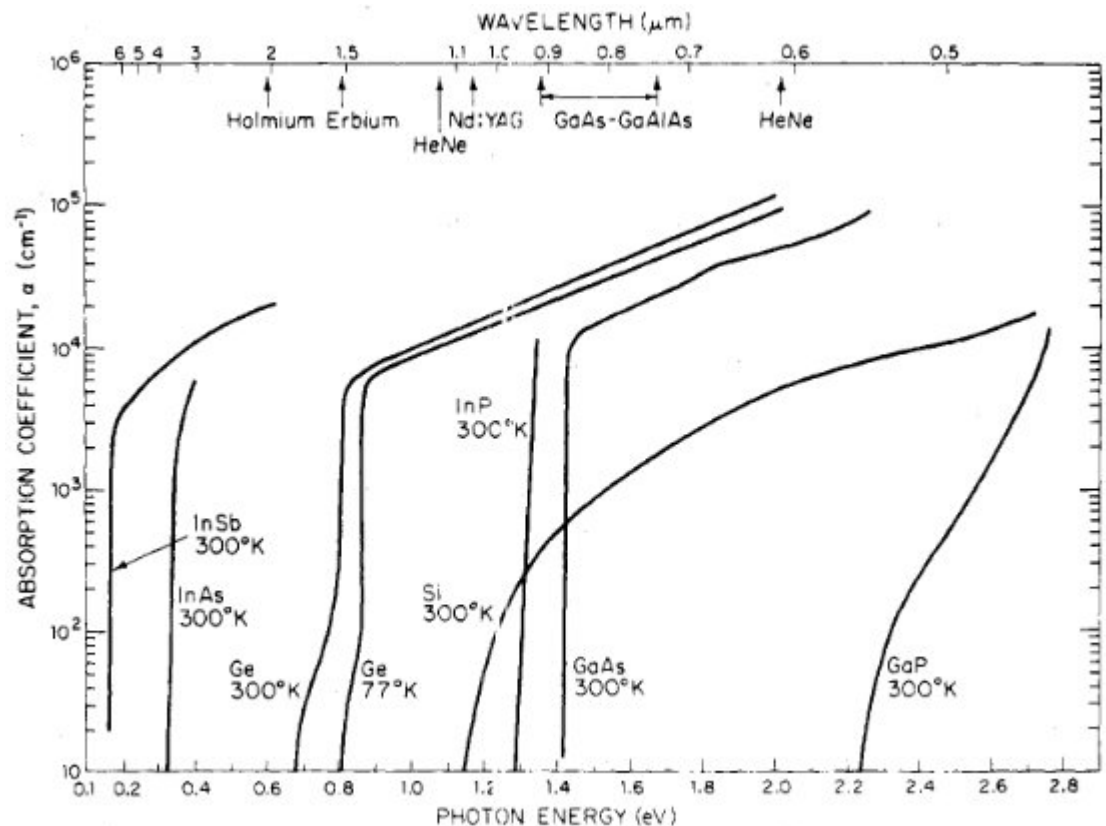


Fig. Optical absorption coefficient for different materials [1]

[1] Provost, J. P., Vallee, G. (1980). *Communications in Mathematical Physics*, 76, 289-301.

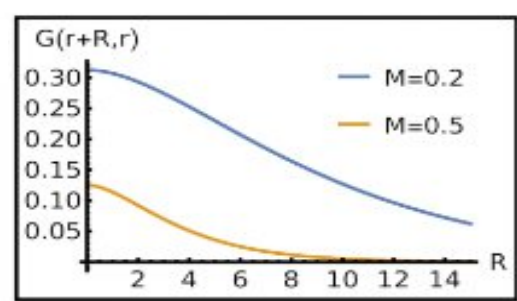
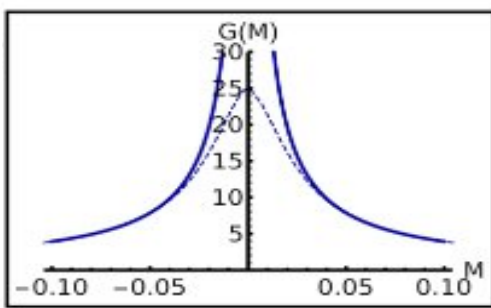
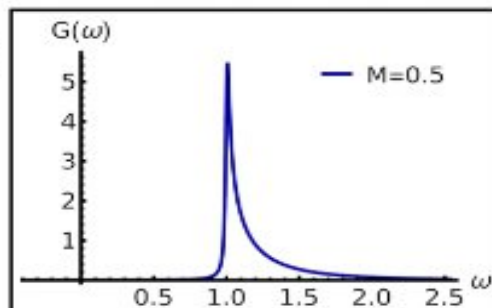
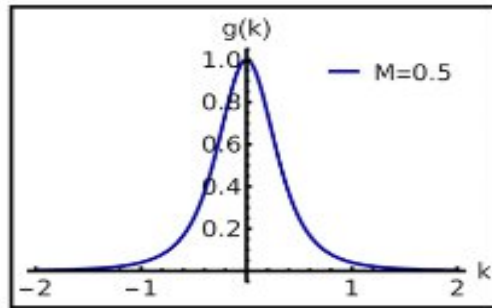
[2] Marzari, N., & Vanderbilt, D. (1997). *Physical review B*, 56(20), 12847.

[3] Souza, I., Wilkens, T., & Martin, R. M. (2000). *Physical Review B*, 62(3), 1666.

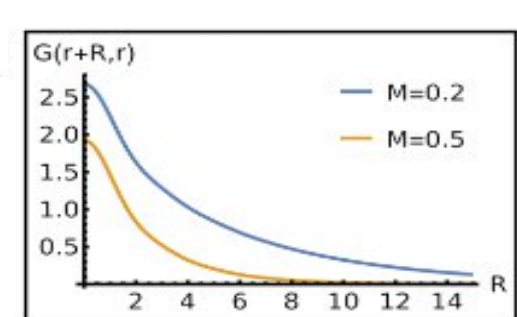
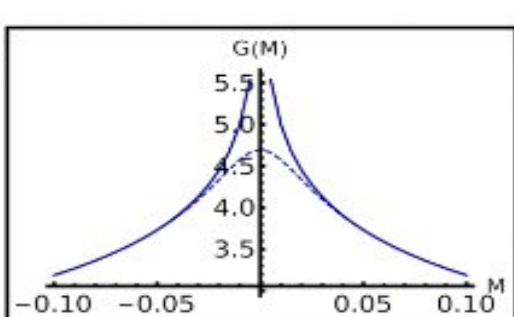
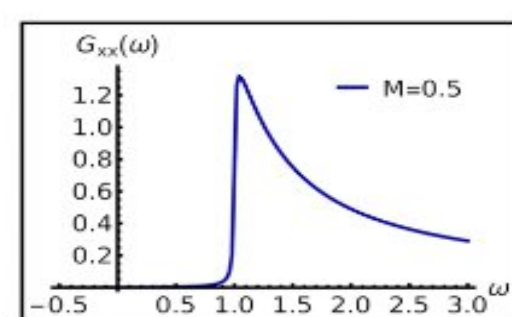
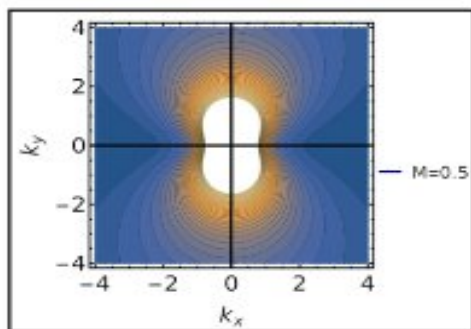
Quantum metric and fidelity number

- Compute quantum metric for different dimensions [1].

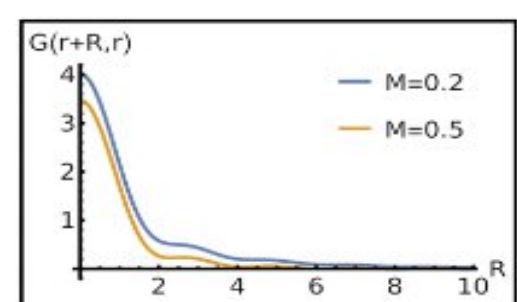
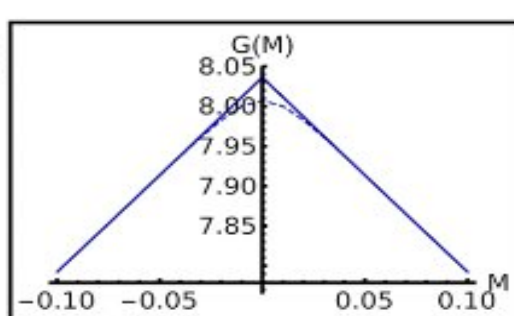
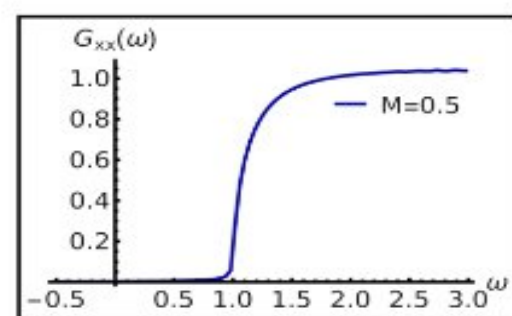
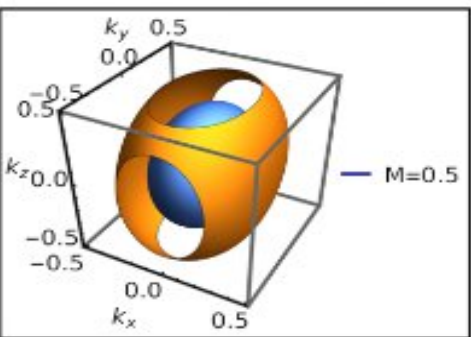
1D



2D



3D



Opacity of Graphene

- For low energy, we can write graphene as a Dirac Hamiltonian

$$H = \hbar v_F (k_x \sigma_x + \eta k_y \sigma_y)$$

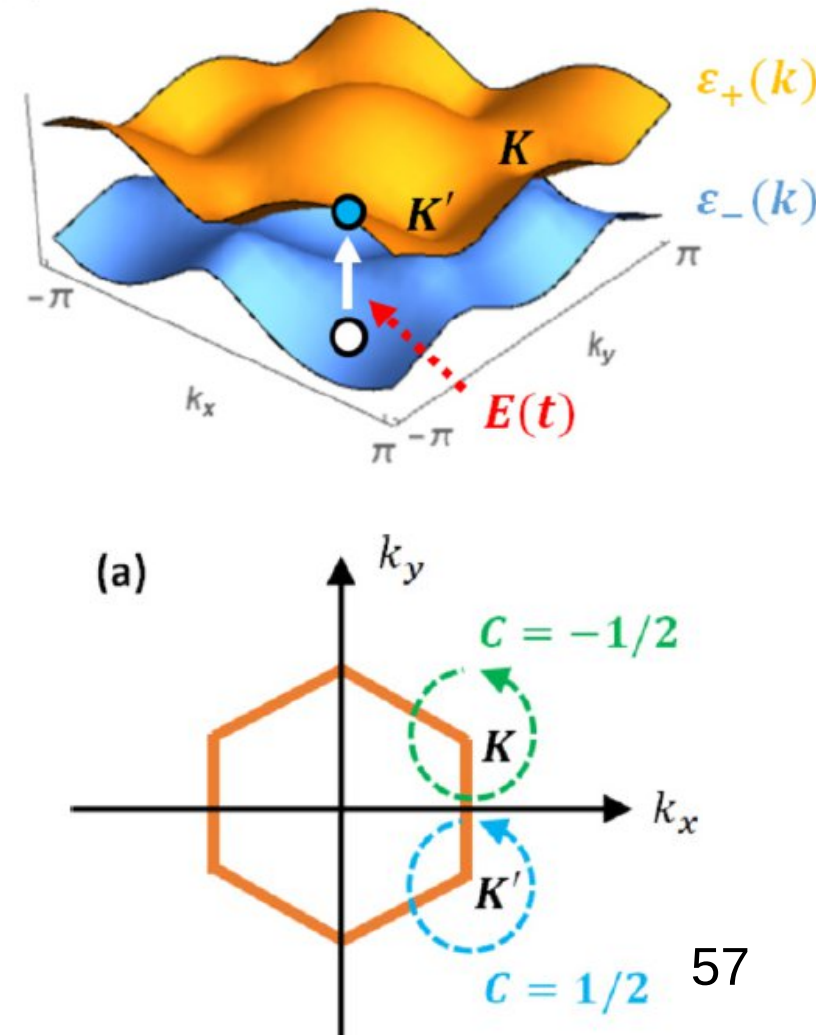
- And moreover, calculate the topological charge

$$\oint \frac{d\varphi}{2\pi} \langle -\eta | i\partial_\varphi | -\eta \rangle = -c\eta$$

- The azimuthal quantum metric is the topological charge squared

$$g_{\varphi\varphi}(\mathbf{k}) = C^2 \eta^2 \quad \text{"Metric-curvature correspondence [1]"}$$

[1] von Gersdorff, G., & Chen, W. (2021). *Physical Review B*, 104(19), 195133.



Opacity of Graphene

- For low energy, we can write graphene as a Dirac Hamiltonian

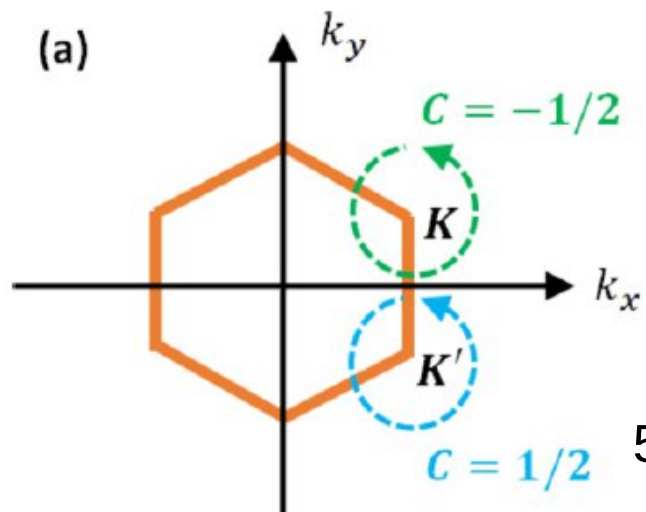
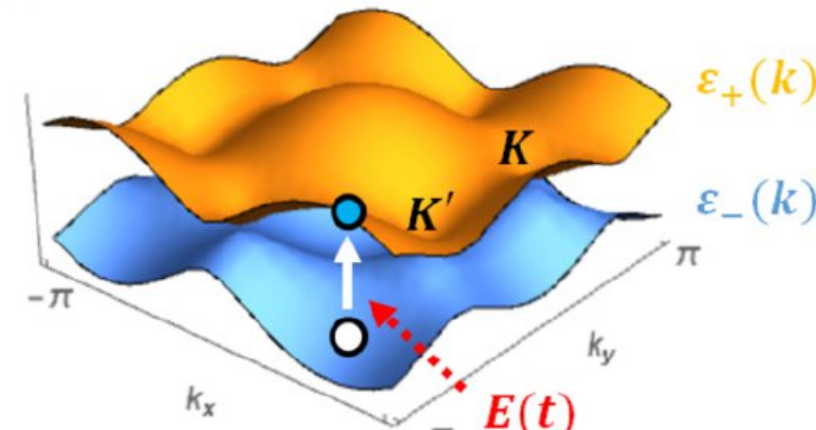
$$H = \hbar v_F (k_x \sigma_x + \eta k_y \sigma_y)$$

- And moreover, calculate the topological charge

$$\oint \frac{d\varphi}{2\pi} \langle -\eta | i\partial_\varphi | -\eta \rangle = -c\eta$$

- In Cartesian coordinates

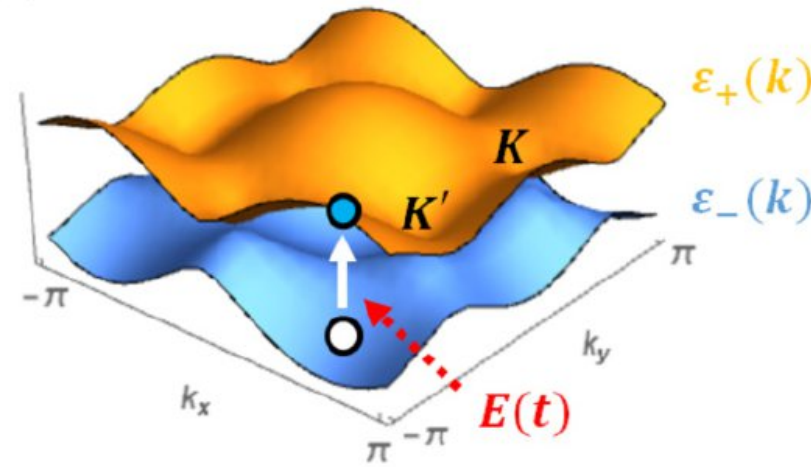
$$g_{xx} = \frac{\sin^2 \varphi}{k^2} g_{\varphi\varphi}$$



Opacity of Graphene

We now proceed to calculate the opacity

$$P = \frac{W_a}{W_i}$$



Opacity of Graphene

We now proceed to calculate the opacity

$$P = \frac{W_a}{W_i}$$

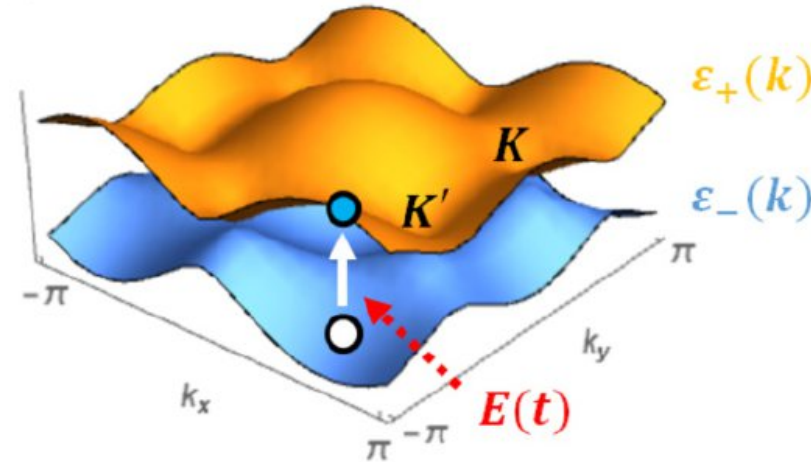
← “Incidence power”

Considering a planar wave

$$\mathbf{S} = \frac{c}{4\pi} E^2 \hat{\mathbf{x}}$$

The incidence power will be

$$W_i = \frac{c}{4\pi} E^2$$



Opacity of Graphene

We now proceed to calculate the opacity

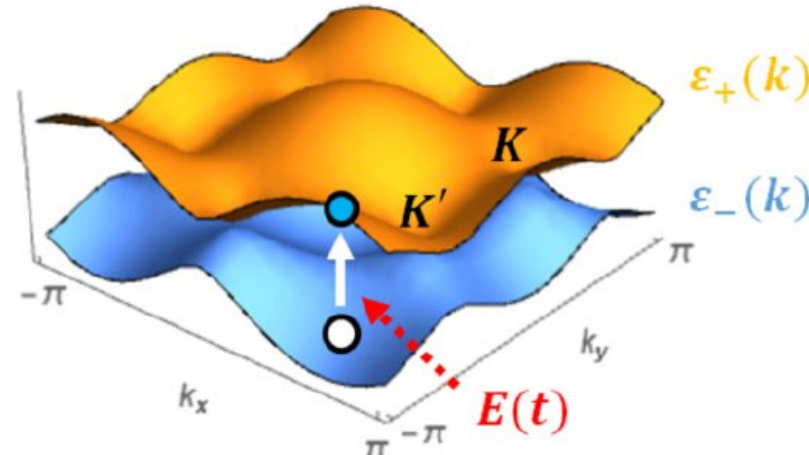
$$P = \frac{W_a}{W_i} \quad \text{“Absorption power”}$$

Using Fermi's golden rule

$$\Gamma_k = \frac{2\pi}{\hbar} |\langle n | qE_0 \partial_x | m \rangle|^2 \delta(\hbar\omega + \varepsilon_n - \varepsilon_m)$$

$$= \frac{2\pi}{\hbar} q^2 E_0^2 g_{xx} \delta(\hbar\omega + \varepsilon_n - \varepsilon_m)$$

$$= \frac{2\pi}{\hbar} q^2 E_0^2 \frac{\sin^2 \varphi}{k^2} g_{\varphi\varphi} \delta(\hbar\omega - 2\hbar v_F k)$$



Opacity of Graphene

We now proceed to calculate the opacity

$$P = \frac{W_a}{W_i}$$

“Absorption power”

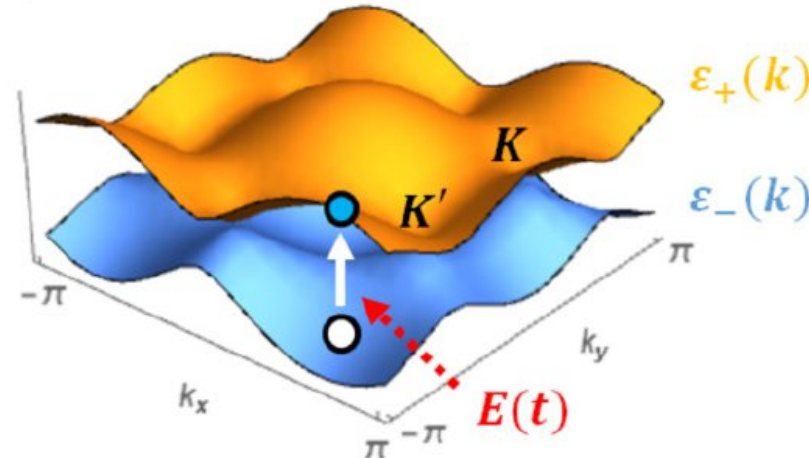
Using Fermi's golden rule

$$\Gamma_k = \frac{2\pi}{\hbar} |\langle n | qE_0 \partial_x | m \rangle|^2 \delta(\hbar\omega + \varepsilon_n - \varepsilon_m)$$

$$= \frac{2\pi}{\hbar} q^2 E_0^2 g_{xx} \delta(\hbar\omega + \varepsilon_n - \varepsilon_m)$$

$$= \frac{2\pi}{\hbar} q^2 E_0^2 \frac{\sin^2 \varphi}{k^2} g_{\varphi\varphi} \delta(\hbar\omega - 2\hbar v_F k)$$

Quantum metric appears



Opacity of Graphene

We now proceed to calculate the opacity

$$P = \frac{W_a}{W_i} \quad \text{“Absorption power”}$$

The total of absorption events per time is

$$\eta = \int \frac{d^2\mathbf{k}}{(2\pi)^2} \Gamma_{\mathbf{k}} = \frac{q^2 E_0^2 g_{\varphi\varphi}}{\hbar^2 \omega}$$

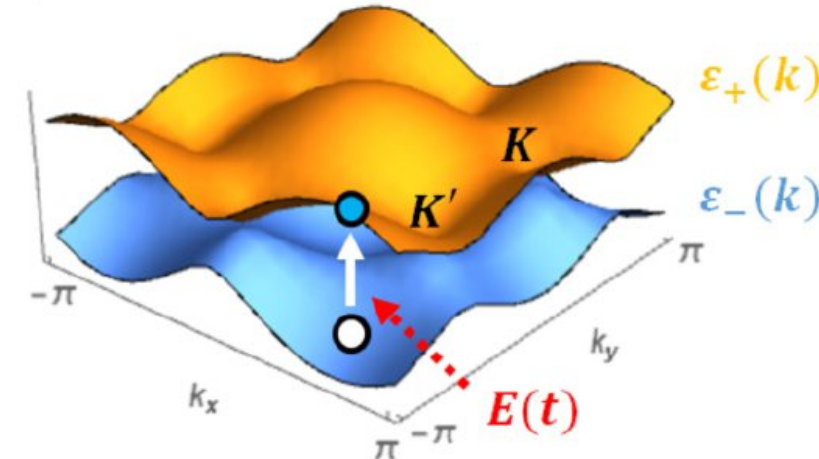
We recover the famous opacity of graphene [2]

$$P = \pi \alpha \times 4g_{\varphi\varphi} = 2.3\% \times 4g_{\varphi\varphi}$$

[1] von Gersdorff, G., & Chen, W. (2021). *Physical Review B*, 104(19), 195133.

[2] Sheehy, D. E., & Schmalian, J. (2009). *Physical Review B*, 80(19), 193411.

[3] de Sousa, M. S., Cruz, A. L., & Chen, W. (2023). *arXiv preprint arXiv:2303.14549*.



Opacity of Graphene

We now proceed to calculate the opacity

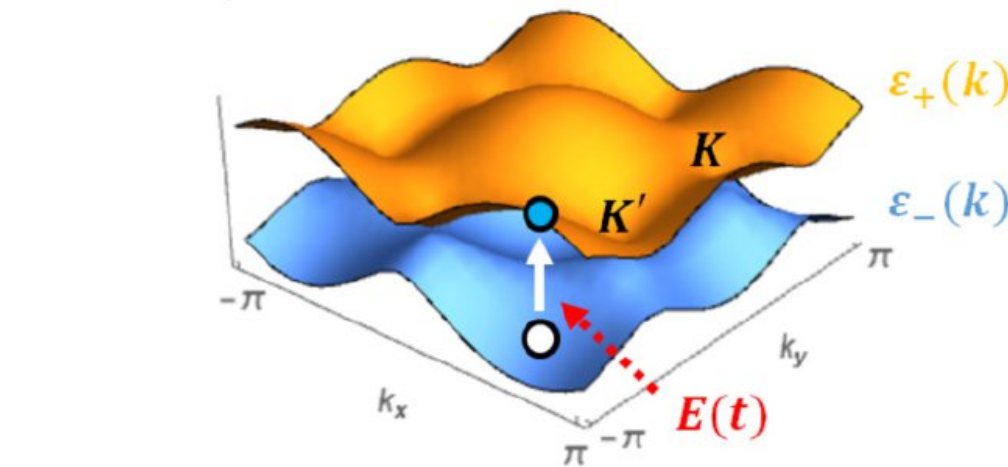
$$P = \frac{W_a}{W_i} \quad \text{“Absorption power”}$$

The total of absorption events per time is

$$\eta = \int \frac{d^2\mathbf{k}}{(2\pi)^2} \Gamma_{\mathbf{k}} = \frac{q^2 E_0^2 g_{\varphi\varphi}}{\hbar^2 \omega}$$

We recover the famous opacity of graphene [2]

$$P = \pi \alpha \times 4g_{\varphi\varphi} = 2.3\% \times 4g_{\varphi\varphi}$$



The topological charge
is hidden

[1] von Gersdorff, G., & Chen, W. (2021). *Physical Review B*, 104(19), 195133.

[2] Sheehy, D. E., & Schmalian, J. (2009). *Physical Review B*, 80(19), 193411.

[3] de Sousa, M. S., Cruz, A. L., & Chen, W. (2023). *arXiv preprint arXiv:2303.14549*.

Conclusion

- Graphene can manipulated to create different electronic properties
- In GNRs with RSOC and magnetization we can manipulate equilibrium currents with gate voltage.
- We can create NLSM by introducing vacancies, and these are robust to perturbations
- With vacancy engineering, we can generically create ZEFB, which could lead to interesting phenomena.
- The quantum metric provides us with additional tools to study topology and has experimental significance, such as in optical conductivity.